

Toward more efficient heuristic construction of Boolean functions

Domagoj Jakobovic^a, Stjepan Picek^b, Marcella S. R. Martins^c, Markus Wagner^d

^a*University of Zagreb - Croatia*

^b*Delft University of Technology - The Netherlands*

^c*Federal University of Technology - Parana, Brazil*

^d*University of Adelaide - Australia*

Abstract

Boolean functions have numerous applications in domains as diverse as coding theory, cryptography, and telecommunications. Heuristics play an important role in the construction of Boolean functions with the desired properties for a specific purpose. However, there are only sparse results trying to understand the problem's difficulty. With this work, we aim to address this issue. We conduct a fitness landscape analysis based on Local Optima Networks (LONs) and investigate the influence of different optimization criteria and variation operators. We observe that the naive fitness formulation results in the largest networks of local optima with disconnected components. Also, the combination of variation operators can both increase or decrease the network size. Most importantly, we observe correlations of local optima's fitness, their degrees of interconnection, and the sizes of the respective basins of attraction. This can be exploited to restart algorithms dynamically and influence the degree of perturbation of the current best solution when restarting.

Keywords:

balancedness, nonlinearity, landscape analysis, local optima networks

Email addresses: domagoj.jakobovic@fer.hr (Domagoj Jakobovic),
s.picek@tudelft.nl (Stjepan Picek), marcella@utfpr.edu.br (Marcella S. R.
Martins), markus.wagner@adelaide.edu.au (Markus Wagner)

1. Introduction

Boolean functions are mathematical objects that can be uniquely represented in truth tables and they have applications in diverse domains. Not only do they form a core concept in combinatorial optimization, such as in the satisfiability problem, but they are used to construct Hadamard matrices [1], strongly regular graphs [2], and decision diagrams [3]. In coding theory, every binary unrestricted code of length 2^n can be interpreted as a set of Boolean functions [4, 5]. In sequences, bent sequences constructed using bent Boolean functions have the lowest value of mutual correlations and autocorrelations, and they are used in communication systems with multiple access [6]. In telecommunications, bent Boolean functions are used in CDMA networks [7]. In cryptography, Boolean functions are used in stream and block ciphers as the source of nonlinearity [8, 9], the design of hash functions [10], or for generating pseudorandom numbers [11]. While various domains have different usages of Boolean functions, some shared characteristics remain. For instance, the ratio between the zeros and ones in the Boolean function's truth table is an important characteristic for many fields. Similarly, the nonlinearity property is not only relevant in cryptography, but also coding theory and sequences. Unfortunately, such widespread use of Boolean functions can also represent a problem since there are numerous scenarios (e.g., considering Boolean function size or relevant properties) for Boolean functions, and it is not always readily available how to construct the required Boolean function.

There are several construction methods to construct Boolean functions: algebraic constructions, random search, heuristics, and combinations of those methods [12]. The advantages of heuristics seem to be (1) the ability to generate many different functions, (2) easy adjustment for different criteria, and (3) very good performance if the size of a Boolean function is not too large. On the other hand, the main drawbacks are (1) no guarantee that optimal solutions will be reached, (2) for every new Boolean function size, new optimization needs to be undertaken, and (3) due to the huge search space size, heuristics are limited in the Boolean function size. In practice, in many domains, the size n of a Boolean function is not very large. For instance, in error-correcting codes, the sizes usually do not surpass 10 since they already give codes of size 2^n (i.e., codes of length 1 024). In cryptography, when used as vectorial Boolean functions, they rarely surpass the size 8, and in the stream ciphers, the size was at most 10 until recent algebraic attacks, and now, the size goes up to 20 inputs. At the same time, already for $n > 5$,

38 the exhaustive search is not possible. Note, that, for a Boolean function with
 39 n inputs, there are 2^{2^n} possible Boolean functions.

40 Heuristics is applied to evolve Boolean functions for cryptography [13] and
 41 combinatorial designs [14, 15]. What is more, some of the common properties
 42 of Boolean functions commonly evolved with heuristics are relevant in the
 43 telecommunications [7] and sequences [6] domains. Thus, while heuristics has
 44 an important role in the design of Boolean functions, there are only sparse
 45 results trying to understand the problem’s difficulty or when it can reach
 46 optimal solutions. Fitness landscape analysis (FLA) studies the influence
 47 of representations on the design of such heuristics, addressing the relative
 48 importance of features in explaining the algorithm performance [16].

49 This article investigates how a range of different design decisions can affect
 50 the search for Boolean functions. In particular, we conduct the first FLA for
 51 Boolean functions considering several function sizes most occurring in the
 52 literature, Boolean function properties, and variation operators in isolation
 53 as well as in combination. As far as we know, this is also the first time that
 54 combined neighborhood strategies are applied (in parallel) and considered in
 55 an FLA context in general.

56 2. Boolean Functions and Their Properties

57 Let n be a positive integer, i.e., $n \in \mathbb{N}^+$. The set of all n -tuples of elements
 58 in the field \mathbb{F}_2 is denoted as \mathbb{F}_2^n where \mathbb{F}_2 is the Galois field with two elements.
 59 The inner product of two vectors a and b is denoted by $a \cdot b$ and equals
 60 $a \cdot b = \bigoplus_{i=0}^{n-1} a_i b_i$. Here, “ \oplus ” represents addition modulo two (bitwise XOR).

61 An $(n, 1)$ -function is any mapping f from \mathbb{F}_2^n to \mathbb{F}_2 and such a function
 62 is called the Boolean function. A Boolean function f on \mathbb{F}_2^n can be uniquely
 63 represented by a truth table (TT), which is a vector $(f(0), \dots, f(1))$ that
 64 contains the function values of f , ordered lexicographically, i.e., $a \leq b$.

65 The Walsh-Hadamard transform W_f is a unique representation of a
 66 Boolean function that measures the correlation between $f(x)$ and the lin-
 67 ear functions $a \cdot x$ [17]:

$$W_f(a) = \sum_{x \in \mathbb{F}_2^n} (-1)^{f(x) \oplus a \cdot x}. \quad (1)$$

68 A Boolean function f is *balanced* if it takes the value 1 exactly the same
 69 number 2^{n-1} of times as the value 0 when the input ranges over \mathbb{F}_2^n .

x_2	x_1	x_0	TT
0	0	0	1
0	0	1	1
0	1	0	0
0	1	1	1
1	0	0	0
1	0	1	0
1	1	0	1
1	1	1	0

Table 1: Truth table of a Boolean function with 3 inputs.

70 The minimum Hamming distance between a Boolean function f and all
71 affine functions (in the same number of variables as f) is called the nonlin-
72 earity of f . The nonlinearity Nl_f of a Boolean function f can be expressed
73 in terms of the Walsh-Hadamard coefficients as [17]:

$$Nl_f = 2^{n-1} - \frac{1}{2} \max_{a \in \mathbb{F}_2^n} |W_f(a)|. \quad (2)$$

74 In Table 1, we give an example of a Boolean function with 3 inputs.
75 Clearly, this function is balanced as it has the same number of zeros and
76 ones in the truth table representation (TT column).

77 In Table 2, we give an example of Walsh-Hadamard calculation of the
78 Boolean function from Table 1. Notice that to conform with Eq. (1), instead
79 of TT, we write $f(x)$. Also, while we write a values as integers, they should
80 be considered as binary values. Finally, from column $W_f(a)$, we see that the
81 maximal absolute Walsh-Hadamard spectrum value equals 4, which means
82 that nonlinearity equals 2 as per Eq. (2) ($2^2 - \frac{1}{2} \cdot 4 = 2$).

83 The maximal value of the Walsh-Hadamard spectrum equals at least $2^{n/2}$,
84 which occurs in the case of bent Boolean functions [1]. Bent functions cannot
85 be balanced, as their Hamming weight equals $2^n - 1 \pm 2^{\frac{n}{2}-1}$. Bent functions
86 exist only for n even. The nonlinearity of bent functions equals [1, 18]:

$$Nl_f = 2^{n-1} - 2^{\frac{n}{2}-1}. \quad (3)$$

87 The nonlinearity of a Boolean function with n variables is bounded above
88 by $2^{n-1} - 2^{\frac{n}{2}-1}$ (the Covering Radius Bound). Clearly, this bound cannot be

a	$f(x)$	$W_f(a)$
0	1	$(-1)^1 + (-1)^1 + (-1)^0 + (-1)^1 + (-1)^0 + (-1)^0 + (-1)^1 + (-1)^0 = 0$
1	1	$(-1)^1 + (-1)^0 + (-1)^0 + (-1)^0 + (-1)^0 + (-1)^1 + (-1)^1 + (-1)^1 = 0$
2	0	$(-1)^1 + (-1)^1 + (-1)^1 + (-1)^0 + (-1)^0 + (-1)^0 + (-1)^0 + (-1)^1 = 0$
3	1	$(-1)^1 + (-1)^0 + (-1)^1 + (-1)^1 + (-1)^0 + (-1)^1 + (-1)^0 + (-1)^0 = 0$
4	0	$(-1)^1 + (-1)^1 + (-1)^0 + (-1)^1 + (-1)^1 + (-1)^1 + (-1)^0 + (-1)^1 = -4$
5	0	$(-1)^1 + (-1)^0 + (-1)^0 + (-1)^0 + (-1)^1 + (-1)^0 + (-1)^0 + (-1)^0 = 4$
6	1	$(-1)^1 + (-1)^1 + (-1)^1 + (-1)^0 + (-1)^1 + (-1)^1 + (-1)^1 + (-1)^0 = -4$
7	0	$(-1)^1 + (-1)^0 + (-1)^1 + (-1)^1 + (-1)^1 + (-1)^0 + (-1)^1 + (-1)^1 = -4$

Table 2: Calculation of the Walsh-Hadamard spectrum for a Boolean function with 3 inputs.

89 tight when n is odd, so for Boolean functions with an odd number of inputs,
90 the maximal nonlinearity lies between $2^{n-1} - 2^{\frac{n-1}{2}}$ and $2^{n-1} - 2^{\frac{n}{2}-1}$.

91 While we consider here only two properties, balancedness and nonlinear-
92 ity, they play important roles in different domains. For example, finding the
93 covering radius for the Reed-Muller code of order one is equivalent to find-
94 ing maximally nonlinear Boolean functions [17]. Note that balanced Boolean
95 functions are used in cryptography and coding theory while bent functions
96 are, for instance, used in sequences and mobile networks.

97 3. Applications of Boolean Functions

98 In the last few decades, there has been a number of papers considering
99 heuristics and Boolean functions. A more careful study reveals that a large
100 part of those works considers applications in cryptography, and we provide
101 an overview in the following.

102 To the best of our knowledge, Millan et al. were the first to apply ge-
103 netic algorithms (GAs) to the evolution of cryptographically suitable Boolean
104 functions [19]. There, the authors experimented with GA to evolve Boolean
105 functions with high nonlinearity. Later, Millan et al. [20] continued to use
106 GA to evolve Boolean functions with high nonlinearity. In conjunction with
107 the GA, they used hill climbing and a resetting step to find Boolean func-
108 tions with even higher nonlinearity and sizes of up to 12 inputs. Dawson et
109 al. [21] experimented with two-stage optimization to generate Boolean func-
110 tions. They used a combination of simulated annealing and hill-climbing with
111 a cost function motivated by the Parseval theorem to find functions with high
112 nonlinearity and low autocorrelation. Kavut and Melek [22] developed im-
113 proved cost functions for a search that combines simulated annealing and hill

114 climbing. With that approach, the authors were able to find some functions
115 of eight and nine inputs that have a combination of nonlinearity and auto-
116 correlation values previously not obtained. Millan et al. [23] proposed a new
117 adaptive strategy for the local search algorithm for the generation of Boolean
118 functions with high nonlinearity. Hernan et al. [24] were the first to use a
119 multi-objective random bit climber to search for balanced Boolean functions
120 of size up to eight inputs with high nonlinearity. Picek et al. [25] experimented
121 with genetic algorithms and genetic programming to find Boolean functions
122 that possess several cryptographic properties. As far as we are aware, this
123 is the first application of genetic programming to the evolution of Boolean
124 functions with cryptographic properties. ~~Picek et al. investigated the sym-~~
125 ~~metries in highly nonlinear balanced Boolean functions with 8 inputs [26].~~
126 Mariot and Leporati [27] used Particle Swarm Optimization to find Boolean
127 functions with good trade-offs of cryptographic properties for dimensions up
128 to 12.

129 There have been several successful approaches where the authors could
130 find bent Boolean functions for different dimensions. Hrbacek and Dvorak
131 experimented with Cartesian genetic programming to evolve bent Boolean
132 functions of size up to 16 inputs [30]. ~~Picek and Jakobovic used genetic pro-~~
133 ~~gramming to evolve algebraic constructions used to construct bent Boolean~~
134 ~~functions [31].~~

135 When considering combinatorial designs, Mariot et al. used evolution-
136 ary algorithms to design binary orthogonal arrays [14] and orthogonal Latin
137 squares [15].

138 4. Analyzing Fitness Landscapes

139 Fitness landscapes describe the relationship between search and fitness
140 space [33], thus a heuristic strategy can navigate a specific landscape struc-
141 ture searching for optimal solutions.

142 Several cost models have been used to make specific predictions for com-
143 binatorial problems, identifying which features of the fitness landscape con-
144 tribute more to the problem solving complexity during the search. By iden-
145 tifying these features, some improvements regarding the algorithm perfor-
146 mance can be designed.

147 The Local Optima Network (LON) [34] is a model designed to under-
148 stand the local optima structure in combinatorial landscapes, incorporating

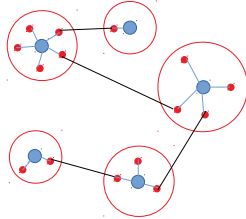


Figure 1: An example of the connectivity in local optima networks.

149 network analysis techniques to study fitness landscapes and problem diffi-
 150 culty [35].

151 The fitness landscape in LON models is modeled as a graph where the
 152 local optima represent nodes that can be connected. A local search heuristic
 153 \mathcal{H} maps the solution space S to the set of locally optimal solutions S^* . Given
 154 a fitness function F , a solution i in the solution space S is a local maximum
 155 according to a neighbourhood operator N if $F(i) \geq F(s), \forall s \in N(i)$.

156 Each local optima i has an associated set of basin of attraction defined
 157 by $B_i = \{s \in S | \mathcal{H}(s) = i\}$. This set contains all the solutions that, after
 158 applying a local search starting from each of them, the procedure returns
 159 i . The cardinality of B_i is the size of the basin of attraction of i . Given a
 160 neighborhood operator, we assume a connection between two local optima if
 161 at least one solution in one basin has a neighbor solution in the other basin.
 162 This assumption is based on previous basin-edges models, which also do not
 163 consider weighted edges [34, 36, 37].

164 Figure 1 shows a simplified LON for visualization purposes, illustrating
 165 the basin of attraction (red circles), their local optima (big blue dots), the
 166 solutions that converge to the local optima when applying the local search
 167 (small red dots), and the edges between the local optima (black lines) that
 168 exist due to neighborhood. Note that sophisticated heuristics might result in
 169 many more interconnections between the basin of attraction than what we
 170 have presented in the example.

171 In early works, local optima networks were exhaustively extracted on
 172 representative NK landscape instances [38, 34]. Additionally, some works
 173 investigated the correlation between LON features and the performance of
 174 search heuristics [39, 40, 16].

175 Permutation-based problems have also been subject to LON analyzes [41].
 176 Besides, [35] extended the LON modeling to neutral fitness landscapes. Neu-
 177 tral networks are connected networks of solutions of equal fitness, with pos-

178 sibly jumps between them. The authors study two neutral versions of the
179 NK landscape model, tuning the amount of neutrality. The results confirmed
180 that the study of neutrality could improve the heuristic search.

181 Recently, some works addressed a LON variant called Compressed Lo-
182 cal Optima Network. The work proposed in [42] investigated fitness land-
183 scape properties for the Number Partitioning Problem, exploring whether the
184 global landscape structure of the number partitioning problem changes with
185 the phase transition. In [43], the authors analyzed the network features to
186 find differences between the landscape structures for the Permutation Flow-
187 shop Scheduling Problem (PFSP). The results provided insights into which
188 features impact the performance of an iterated local search heuristic.

189 The authors in [36] investigated two hill-climbing local search procedures
190 for building their corresponding LONs. The LONs were analyzed to under-
191 stand the difficulty of Travelling Thief Problem (TTP) instances. Among
192 others, they found that certain operators can result in LONs with discon-
193 nected components and that at times potentially exploitable correlations of
194 node degree, basin size, and fitness exist.

195 Using a similar methodology, the first landscape analysis in the greater
196 field of security investigated cryptographic S-Boxes [37]. For the chosen fit-
197 ness functions and two neighbourhood operators (considered in isolation), it
198 was observed that the number of local optima is substantial, and a conjec-
199 ture has been made that links S-Boxes of odd dimensions to their problem
200 difficulty.

201 Here, we use fitness landscape analysis to study the effects that algorithmic
202 design decisions have on optimizing Boolean functions' two important
203 properties. We consider three fitness functions, two initialization strategies,
204 and three neighborhood operators – the latter in isolation and combination,
205 resulting in seven different neighborhoods.

206 5. Creating Networks with Local Search

207 In order to obtain LONs of the Boolean function optimization landscape,
208 we use a local search procedure that, starting from a given initial solution,
209 converges to a corresponding local optimum. Along with the initial solution,
210 all the intermediate solutions leading from the initial solution to the local op-
211 timum are added as the members of that local optimum's basin of attraction.
212 This procedure is repeated for each solution in the set of initial solutions. Af-
213 ter that, we record all unique local optima and reconstruct the connections

Algorithm 1 A greedy local search heuristic

```
1:  $s \leftarrow$  initial solution
2: while there is an improvement do
3:    $s^* = s$ 
4:   for each  $s^{**}$  in  $\mathcal{N}(s)$  do
5:     if  $F(s^{**}) > F(s^*)$  then
6:        $s^* \leftarrow s^{**}$ 
7:     end if
8:   end for
9:    $s = s^*$ 
10: end while
```

214 between their basins of attraction.

215 The local search is described in Algorithm 1; it can be used with an
216 arbitrary representation and an arbitrary neighborhood relationship, where
217 $\mathcal{N}(\cdot)$ represents the neighborhood of the given solution. In the local search,
218 a new solution is accepted only if at least one solution with a better fitness
219 value is found within the entire neighborhood. Note that the algorithm is
220 deterministic; if there are multiple solutions with the same fitness value,
221 the algorithm will retain the first one that it encounters, while the ordering
222 of the solutions in the neighborhood depends on the actual neighborhood
223 relation. If no better solution is found in the initial solution neighborhood,
224 the algorithm will not record the initial solution as a local optimum.

225 5.1. Neighborhood Operators

226 This study considers the truth table representation of Boolean functions,
227 which is encoded as a bitstring. We opted to use the bitstring encoding,
228 even though the related works usually report graph/tree encoding as the
229 best performing one, due to two reasons. First, the properties we consider in
230 our fitness functions are directly connected with the truth table representa-
231 tion. Consequently, exploring neighborhoods in the bitstring encoding gives
232 a direct insight into the difficulty of the problem. Contrary, having a small
233 change in an encoding like the tree encoding, which represents a Boolean
234 function in the form of an expression, can cause a large change in the truth
235 table, thus making the algorithmic design decisions more difficult. Second,
236 we explore Boolean functions up to dimension 7 (i.e., when the search space
237 is 2^{128}) and related works show that for such sizes, the bitstring encoding
238 achieves the same performance [13].

239 With the bitstring encoding, we use three neighborhood variants within
240 Algorithm 1:

- 241 1. The first (denoted “swap”) uses the swap operation (also known as
242 “toggle”) to generate the neighborhood; the swap operation takes two
243 different positions in the bitstring and exchanges them.
- 244 2. The second variant (denoted “flip”) flips the selected bit in the bit-
245 string.
- 246 3. The third variant (denoted “insert”) uses the *insertion* operator; this
247 operator takes a value out of the bitstring at a random position i and
248 inserts it at another random position j , thus pushing the values between
249 i and j by one spot to the right.

250 Also, to investigate complementary capabilities, we consider the following
251 four combined neighborhoods: (1) swap/flip, (2) swap/insert, (3) flip/insert,
252 and (4) swap/flip/insert. Whenever we consider any of these, e.g., swap/flip,
253 we first construct the neighborhood for each operator in isolation, then merge
254 them in the defined order (e.g., all the swap neighbors first, then all the insert
255 neighbors), and then consider this sorted sequence as the combined neighbor-
256 hood that is created by considering both operators at the same time. Some
257 authors also considered combined strategies by proposing algorithms that
258 use local search methods based on combined neighborhood operators [44].
259 However, they apply local search strategies sequentially, differently from our
260 investigation: here, in each algorithm step we merge the solutions obtained
261 simultaneously from all operators separately.

262 As we always consider the entire neighborhood before selecting the best,
263 the order of the neighborhood-operators in these combinations does not mat-
264 ter, unless – as previously highlighted – the fitness of several solutions is
265 identical. In that case, the algorithm will keep the first solution with the
266 best fitness value it encounters, which favors first neighborhoods in the com-
267 bination.

268 5.2. Initialization Strategies

269 In preliminary experiments, we observed that randomly sampled initial
270 solutions for the subsequent hill-climbs result in very few edges in the final
271 LONs. To give us a greater chance of observing connections in the LONs, and
272 also for a more systematic approach, we consider “lexicographic” sampling
273 (abbreviated: “lex”). This also starts with a random sample, but all subse-
274 quent samples continue in lexicographic order from the first sample, based
275 on the binary representation.

276 *5.3. Fitness Functions for Optimization of Boolean Functions*

277 The first fitness function uses the nonlinearity value where the goal is to
 278 maximize it:

$$fitness_1 : Nl_f. \quad (4)$$

279 In the second fitness function, we aim to search for balanced, highly non-
 280 linear functions. We use a two-stage fitness in which a fitness bonus equal to
 281 the nonlinearity is awarded only to a perfectly balanced function; otherwise,
 282 the fitness is only described by the balancedness penalty. The balancedness
 283 penalty BAL is defined as the difference up to the balancedness (i.e., the
 284 number of bits that need to be changed to reach balancedness) This dif-
 285 ference is included in the fitness function with a negative sign to act as a
 286 penalty in maximization scenarios. The delta function $\delta_{BAL,0}$ takes the value
 287 one when $BAL = 0$ and is zero otherwise.

$$fitness_2 : -BAL + \delta_{BAL,0} \cdot Nl_f. \quad (5)$$

288 Finally, the third fitness function extends the second one to consider the
 289 whole Walsh-Hadamard spectrum and not only its extreme value:

$$fitness_3 : -BAL + \delta_{BAL,0} \cdot (Nl_f + Indicator). \quad (6)$$

290 The *Indicator* property is the normalized number of occurrences of the max-
 291 imal nonlinearity value in the whole spectrum (denoted $\#max_values$). Nat-
 292 urally, the smaller the number of such maximal values, the easier it is for the
 293 algorithm to reach the next nonlinearity value: $Indicator = 2^n - \frac{\#max_values}{2^n}$.

294 **6. Results and Discussion**

295 This section analyzes the local optima networks obtained using the local
 296 search heuristic to reveal insights about the search space structure. Further-
 297 more, we study the basins of attraction and their relationship with some
 298 LON properties looking for additional search difficulty information.

299 In our experiments, we explore the following parameters of the search
 300 space, which represent various design decisions that need to be made when
 301 setting up a heuristic search for Boolean functions:

- 302 • Boolean functions of size $4 \leq n \leq 7$;
- 303 • three fitness functions (Equations (4), (5), and (6));
- 304 • two initialization strategies;

- 305 • seven neighbourhood types (based on swap, flip, and insert);
- 306 • number of samples (unique initial solutions).

307 As it is possible to perform an exhaustive search for problem size $n =$
 308 4 – because the total number of solutions is 2^{16} – we build the LONs by
 309 enumerating the search space. In other words, the Algorithm 1 is executed
 310 for every possible initial solution (every Boolean function in $n = 4$ variables).
 311 In larger sizes, we conduct a sampling process using a fixed sample size, which
 312 is the number of unique initial solutions: for each solution, we run Algorithm 1
 313 until no further improvements are possible.¹

314 Note that, because both our fitness functions (nonlinearity, balancedness,
 315 and the Walsh-Hadamard spectrum) and our neighbourhood enumeration
 316 here require fully defined functions (so that we can enumerate the complete
 317 neighbourhood), small structural changes would be necessary to transfer our
 318 approach to partially defined Boolean functions that do not define all 2^n
 319 possible solutions.

320 6.1. Topological Properties of Local Optima Networks

321 In Tables 3 and 4, we show graph properties that are often used for
 322 LON analyses [34]. In particular, we extract the following metrics. n_v and n_e
 323 represent the number of vertices (or nodes) and the number of edges of the
 324 generated LON, respectively. As in many other studies, we do not consider
 325 weights in the edges. z is the average degree. C is the average clustering
 326 coefficient. C_r is the average clustering coefficient of corresponding random
 327 graphs (i.e., random graphs with the same number of vertices and mean
 328 degree). b is the average basin size. l is the average shortest path length
 329 between any two local optima. π is the connectivity, which indicates if the
 330 LON is a connected graph. Finally, S is the number of connected components
 331 (sub-graphs).

332 In Table 3, we report on the exhaustive search for Boolean functions with
 333 size $n = 4$. We compare the three fitness functions $fitness_1$, $fitness_2$, and
 334 $fitness_3$ using the seven neighborhood operators. We find that the number
 335 of vertices (n_v) for $flip$, $swap$ is the same for the three functions, and this
 336 behavior also occurs with $swapflip$ and $swapflipinsert$, which indicates that

¹While it is possible to calculate the fitness values of all 2^{32} solutions in case of $n = 5$, it is not possible to conduct this many hill-climbs, including all neighborhood calculations, which are needed to create the networks.

337 the local optima and the distinct starting points are the same for these oper-
338 ators. However, except for *flip* and *swap* on the three functions, the actual
339 LONs are quite different, with the number of edges (n_e) ranging between
340 about 14 000 and 650 000.

341 The average degrees (z) are higher for combined neighborhoods than for
342 the isolated operators. A higher number of edges (n_e) can also be noted for
343 the combined neighborhoods on *fitness*₂ and *fitness*₃. Besides, the *fitness*₁
344 function results in greater average degree than *fitness*₂ and *fitness*₃. Inter-
345 estingly, the LON consists of only one component for almost all instances
346 for *fitness*₂ and *fitness*₃ (with the exception of *flip* and *swap* for *fitness*₂
347 function). In combination with the observed high mean degree and small min-
348 imum distances between nodes, this can mean that a Tabu Search [45, 46]
349 with restarts or a Memetic Algorithm [47] with built-in local searches, or
350 even an approach with explicit niching might be able to perform well and
351 explore the entire network.

352 Table 4 shows the results using 10 000 lexicographic-ordered samples (i.e.,
353 for $n \geq 5$), where a “sample” refers to a sampled starting point and a sub-
354 sequent deterministic hill-climb. We typically find several hundreds of local
355 optima. This indicates that there is a very large number of local optima in
356 the landscape.²

357 Next, with the clustering coefficient (C) of a node i , we measure how
358 close its neighbors are to being a clique, and it characterizes the extent to
359 which nodes adjacent to node i are connected to each other. This determines,
360 together with l , whether a graph is a small-world network (in which nodes
361 are highly clustered yet the path length between them is small). We can
362 observe in both tables that the LONs show a significantly higher degree of
363 local clustering than their corresponding random graphs (C_r). This means
364 that the local optima are connected in two ways: dense local clusters and
365 sparse interconnections, which can be difficult to find and exploit for all op-
366 erators. Besides this, all connected LONs in both tables have a small minimal
367 path length l on average, i.e., any pair of local optima can be connected by
368 traversing only a few other local optima.5mm]

369 Additionally, for $n = 4$, we briefly investigate the extent to which sampled

²We do not report on the results of the LONs based on random initial solutions (and the subsequent hill-climbs), as these consisted of hundreds or even thousands of disconnected components.

370 landscapes are representative of the entire problem. To do so, we sample the
371 landscapes, extract the graph properties, and calculate the correlations. The
372 resulting graph properties can be seen in Table .6 in the Appendix. Table 5
373 reports the Spearman correlation coefficient between the sampled landscapes
374 and the completely enumerated landscapes. When the correlation is higher
375 than 0.4, then we highlight it in light blue. As one might expect, *random*
376 initialization can be used to roughly estimate of the number of components
377 (S). Generally, for the *lex* initialization, the 10 000 samples results in higher
378 correlations than for the 1 000 case; in some of the later experiments, we still
379 consider 1 000 samples due to the size of the neighborhood. In detail, *lex*
380 shows a high correlation coefficient (with the complete enumeration) for the
381 degree, and it ranges between 0.4 and 0.5 for both clustering coefficient (C)
382 and number of components (S).

Function	Operator	n_v	n_e	z	C	C_r	b	l	π	S
<i>fitness₁</i>	<i>flip</i>	12774	275388	43.1170	0.2672	0.0034	3.4656	—	0	9
	<i>insert</i>	12904	435761	67.5389	0.2771	0.0052	3.5939	—	0	7
	<i>swap</i>	12774	275388	43.1170	0.2672	0.0034	3.4656	—	0	9
	<i>flipinsert</i>	1182	150095	253.9679	0.4945	0.2151	54.7394	1.82	1	1
	<i>swapflip</i>	1176	103700	176.3605	0.4093	0.1500	55.0136	1.92	1	1
	<i>swapflipinsert</i>	1176	174167	296.2024	0.5072	0.2521	55.0136	1.77	1	1
	<i>swapinsert</i>	9806	533767	108.8654	0.2794	0.0111	4.5030	—	0	7
<i>fitness₂</i>	<i>flip</i>	1776	14249	16.0462	0.3082	0.0089	2.0878	—	0	3
	<i>insert</i>	1712	20581	24.0432	0.2956	0.0135	2.1379	3.73	1	1
	<i>swap</i>	1776	14249	16.0462	0.3082	0.0092	2.0878	—	0	3
	<i>flipinsert</i>	10922	471252	86.2941	0.1973	0.0079	6.0004	3.23	1	1
	<i>swapflip</i>	10920	401688	73.5692	0.2265	0.0067	6.0015	3.43	1	1
	<i>swapflipinsert</i>	10920	648497	118.7723	0.1955	0.0109	6.0015	2.94	1	1
	<i>swapinsert</i>	1484	29029	39.1226	0.2638	0.0260	2.3140	2.81	1	1
<i>fitness₃</i>	<i>flip</i>	2292	24305	21.2086	0.2648	0.0089	2.2094	3.79	1	1
	<i>insert</i>	2166	30553	28.2114	0.2604	0.0129	2.2872	3.53	1	1
	<i>swap</i>	2292	24305	21.2086	0.2648	0.0093	2.2094	3.79	1	1
	<i>flipinsert</i>	10082	472850	93.8008	0.2053	0.0093	6.5003	3.08	1	1
	<i>swapflip</i>	10080	398788	79.1246	0.2296	0.0079	6.5016	3.24	1	1
	<i>swapflipinsert</i>	10080	642179	127.4165	0.2012	0.0127	6.5016	2.83	1	1
	<i>swapinsert</i>	1866	47681	51.1050	0.2429	0.0271	2.4952	2.73	1	1

Table 3: General LON and basins’ statistics for Boolean functions size 4. In each row, we show the LON that is the result of conducting a hill-climb from each of the possible 2^{16} unique solutions in the search space. A dash is shown when l cannot be computed as multiple disconnected components exist.

Size	Initialization	Function	Operator	n_v	n_e	z	C	C_*	b	l	π	S	
5	lex	<i>fitness2</i>	<i>flip</i>	730	6272	17.1836	0.0221	13.6356	3.0883	1	1	1	
			<i>insert</i>	260	4377	33.6692	0.4909	3.8577	2.0222	1	1	1	
			<i>swap</i>	145	1960	27.0345	0.5687	6.1172	1.9519	1	1	1	
			<i>flipinsert</i>	382	9569	50.0995	0.5323	13.24	27.0969	1.9449	1	1	1
			<i>swapflip</i>	193	2948	30.5492	0.5772	0.1610	52.6528	1.9664	1	1	1
			<i>swapflipinsert</i>	280	7000	50.0000	0.5756	0.1784	36.6464	1.8604	1	1	1
	<i>fitness3</i>	<i>swapinsert</i>	240	5373	44.7750	0.5505	0.1862	4.1458	1.8633	1	1	1	
		<i>flip</i>	813	8055	19.8155	0.3190	0.0238	12.3456	2.9684	1	1	1	
		<i>insert</i>	251	4355	34.7012	0.4918	0.1413	4.4542	1.9452	1	1	1	
		<i>swap</i>	183	3238	35.3880	0.5245	0.1972	5.3497	1.8835	1	1	1	
		<i>flipinsert</i>	414	11849	57.2415	0.5437	0.1395	25.8527	1.8909	1	1	1	
		<i>swapflip</i>	277	6554	47.3213	0.5370	0.1714	37.6570	1.8891	1	1	1	
6	lex	<i>fitness2</i>	<i>swapflipinsert</i>	352	12190	69.2614	0.5584	30.1477	1.8096	1	1	1	
			<i>swapinsert</i>	255	6363	49.9059	0.5292	0.1951	4.3451	1.8267	1	1	1
			<i>flip</i>	363	3025	16.6667	0.3863	0.0450	27.5840	3	1	1	1
			<i>insert</i>	236	3536	29.9661	0.4187	0.1277	2.3136	2.1369	1	1	1
			<i>swap</i>	62	487	15.7097	0.4982	0.2505	5.9677	1.9334	1	1	1
			<i>flipinsert</i>	314	6550	41.7197	0.4724	0.1327	32.7229	2.0490	1	1	1
	<i>fitness3</i>	<i>swapflip</i>	128	1698	26.5313	0.5045	0.2089	78.8047	1.9382	1	1	1	
		<i>swapflipinsert</i>	221	4404	39.8552	0.5305	0.1815	46.0905	1.9461	1	1	1	
		<i>swapinsert</i>	156	2608	33.4359	0.5128	0.2163	3.0128	1.8864	1	1	1	
		<i>flip</i>	595	4822	16.2084	0.3481	0.0280	17.2185	3.1043	1	1	1	
		<i>insert</i>	163	2283	28.0123	0.5252	0.1816	4.4479	1.9076	1	1	1	
		<i>swap</i>	113	1396	24.7080	0.5608	0.2219	5.9735	1.8254	1	1	1	
7	lex	<i>fitness2</i>	<i>flipinsert</i>	422	9640	45.6872	0.4684	0.1076	26.3436	2.0016	1	1	1
			<i>swapflip</i>	249	4420	35.5020	0.4949	0.1437	43.8153	1.9196	1	1	1
			<i>swapflipinsert</i>	348	9459	54.3621	0.5046	0.1572	32.0920	1.8754	1	1	1
			<i>swapinsert</i>	177	3389	38.2938	0.5402	0.2185	4.7345	1.8073	1	1	1
			<i>flip</i>	512	4223	16.4961	0.3550	0.0329	19.3516	—	0	2	2
			<i>insert</i>	513	7742	30.1832	0.3696	0.0592	2.3294	—	0	2	2
	<i>fitness3</i>	<i>swap</i>	30	154	10.2667	0.5846	0.3326	21.9333	2	1	1	1	
		<i>flip</i>	639	5212	16.3130	0.3201	0.0250	15.7042	—	0	2	2	
		<i>insert</i>	465	7152	30.7613	0.3926	0.0659	6.2839	3	1	1	1	
		<i>swap</i>	75	610	16.2667	0.6362	0.2105	1.4.6267	2	1	1	1	

Table 4: General LON and basins' statistics for 10 000 samples, with the lex initialization. We omit the random initialization, as the LONs always consisted of hundred to thousands of disconnected components. We also omit *fitness₁* here as it has also resulted in disconnected components. For $n = 7$ the results for the combined neighborhoods are missing as they were too large to be computed on our systems. A dash is shown when l cannot be computed as multiple disconnected components exist.

Samples	Initialization	n_v	n_e	z	C	C_r	b	l	π	S
1,000	lex	-0.0623	0.1891	0.8638	0.1670	0.0675	0.2181	-0.2018	0.2582	0.3173
	random	-0.0172	0.2468	0.1955			-0.2335		0.2709	
10,000	lex	-0.1807	0.2073	0.9210	0.5187	0.2338	0.4150	0.1632	0.3920	0.3738
	random	-0.0046	0.3290	0.3451	-0.3966		-0.2441			0.4353

Table 5: Spearman correlation coefficient between exhausted and sampled landscapes for $n = 4$ for both *lex* and *random* initialization with 1000 and 10000 samples. Highlighted values present correlation higher than 0.4

383 Figures 2 to 7 present the obtained networks for Boolean functions with
384 size $n = 4$ to $n = 7$.

385 We can see in Figures 2, 4, and 6 that swap and insert LONs, for example,
386 present local dense connected components for $fitness_1$ function, while, in
387 Figures 3, 5, and 7 for flipinsert, swapflipinsert, swapflip, and swapinsert, for
388 examples, LONs are connected graphs for almost all fitness functions (except
389 in swapinsert for $fitness_1$). The LONs for $n = 5$, $n = 6$, and $n = 7$ with *lex*
390 initialization using 10000 samples are connected graphs for almost all fitness
391 functions and operators. For this reason, we suppressed them in this paper.

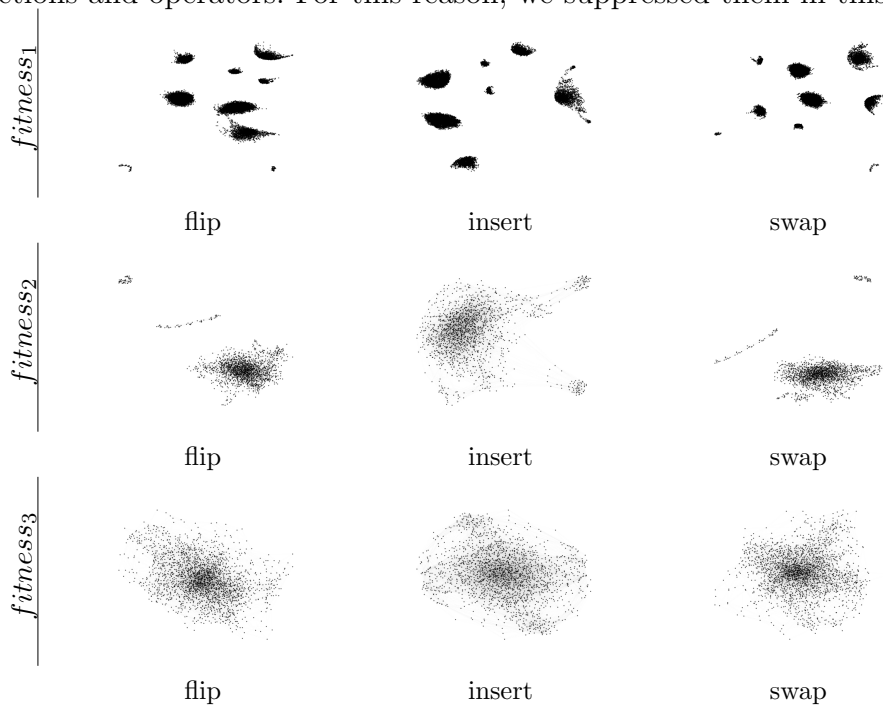


Figure 2: LON graphs on exhaustive $n = 4$ with the three fitness functions for operators flip, insert, swap.

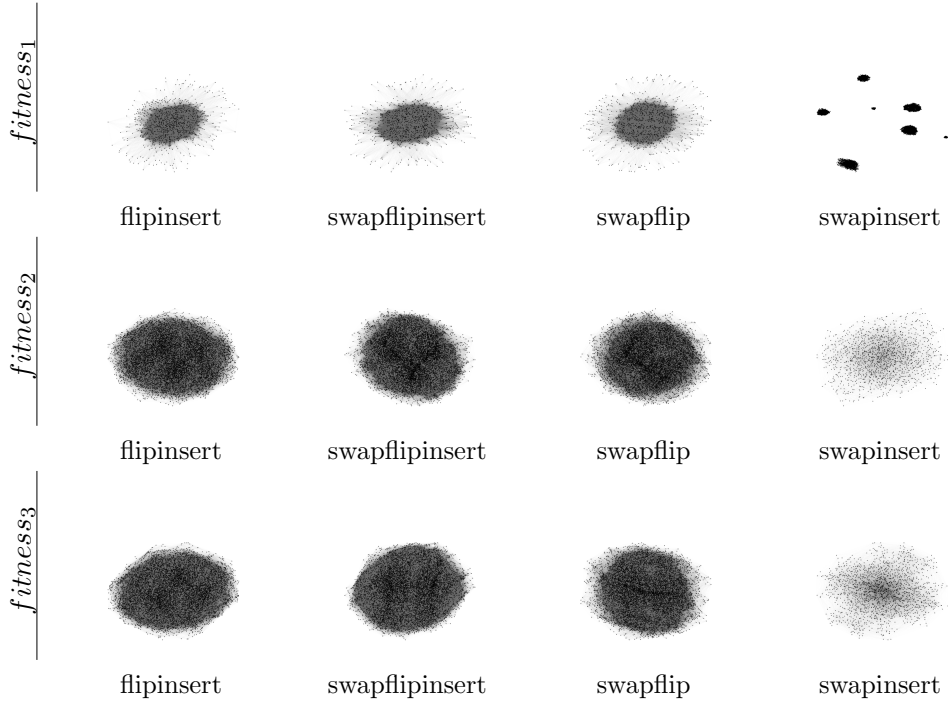


Figure 3: LON graphs on exhaustive $n = 4$ with the three fitness functions for combination using operators flipinsert, swapflipinsert, swapflip, and swapinsert.

392 *6.2. Distribution of Degree*

393 To characterize the networks visually, we provide three types of plots for
 394 our search space: (1) the cumulative degree distribution; (2) the correlation
 395 between the degree of local optima and their corresponding basin sizes; and
 396 (3) the correlation between the fitness of local optima and their corresponding
 397 basin sizes.

398 For the first one, the cumulative degree distribution function represents
 399 the probability $P(k)$ that a random node has a degree larger than k .

400 Let us start with $n = 4$. In the left columns of Figure 8 (for neighborhoods
 401 in isolation) and of Figure 9 (for neighborhoods in combination), we can see
 402 that the degree distributions hardly decay for small degrees for all the three
 403 single operators type and fitness functions, while their dropping rate is very
 404 high for high degrees, presenting short tails to the right. This behavior shows
 405 that there are few nodes with a large number of neighbors. However, most
 406 parts of the local optima have a small number of connections. A benefit of
 407 these few nodes with high connectivity is that these efficiently connect the
 408 entire landscape: a search at a random node has more chances to move to

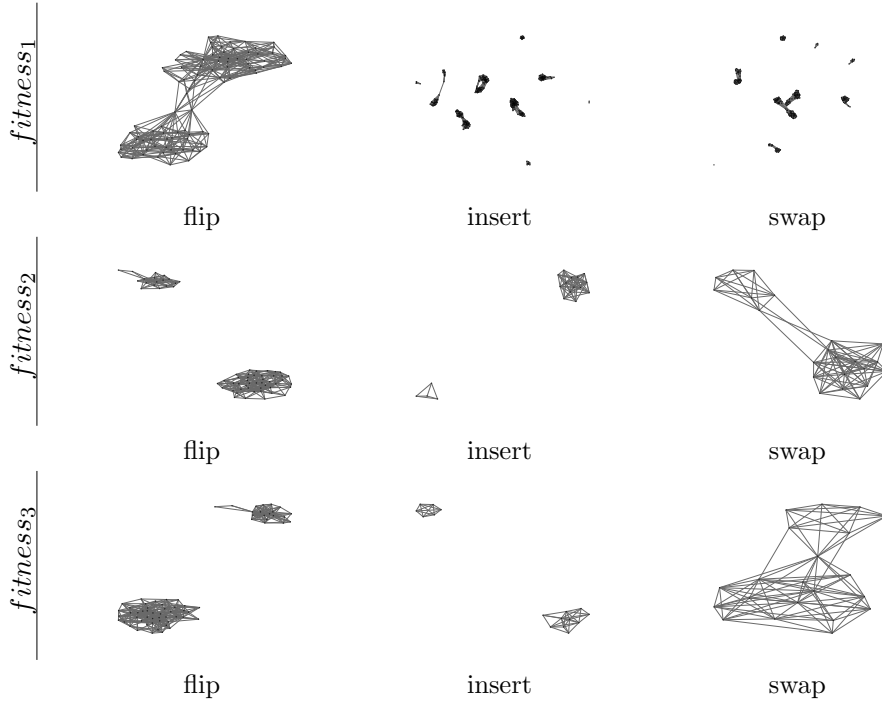


Figure 4: LON graphs for *lex* initialization on $n = 5$ with fitness functions $fitness_1$, $fitness_2$ and $fitness_3$ using 1000 samples for all three operators: flip, insert, swap.

409 one of these high degree nodes, and then to another node, which can be an
 410 efficient way to search the entire network.

411 Local search strategies on networks have been investigated according to
 412 the degree distribution [48], particularly because some real-world network
 413 present properties in the topological structure that can be described by a
 414 power-law, or a scale-free degree distribution $P(k) = k^{-\alpha}$, where $\alpha \in [2, 3]$ is
 415 a scaling parameter.

416 Aiming to study the cumulative degree distribution more strictly, we use
 417 the Kolmogorov-Smirnov test to investigate the adequacy of power-law [49]
 418 and exponential models [50]³. The test is performed on all distributions shown
 419 with a significance level of 0.1. When the *p-value* > 0.1 , the test fails to
 420 reject power-law and exponential as plausible distribution models.

421 Considering the distributions reported in Figure 8 for $n = 4$, none of
 422 them fits power-law nor exponential models. For Figures .13, .14, .15, and .16
 423 (see Appendix) with 1 000 samples, the $n = 6$ instances using lexicographic

³originally proposed by [34] to describe the degree distributions for NK models

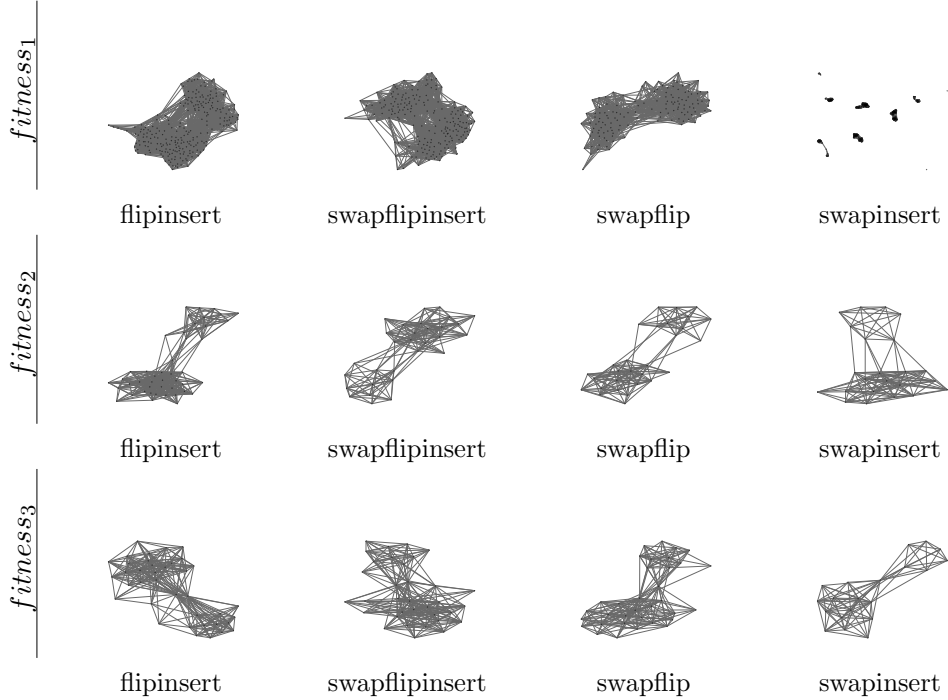


Figure 5: LON graphs for *lex* initialization on $n = 5$ with fitness functions $fitness_1$, $fitness_2$ and $fitness_3$ using 1000 samples for combination using operators flipinsert, swapflipinsert, swapflip, and swapinsert.

424 sampling (*lex*) and $fitness_2$ function type for flip operator, and $fitness_1$
 425 function type for swap operator, fit a power-law. For Figures .17, .18, .19,
 426 and .20 (see Appendix) with 10 000 samples the $n = 5$ instances for $fitness_2$
 427 function type using lexicographic sampling (*lex*) for flip operator fit a power-
 428 law, as well as for the same instance considering the $fitness_3$ function type.
 429 The remaining instances do not fit a power-law nor an exponential model.

430 The degree distribution contributes to search a power-law graph more
 431 rapidly, assuming that the number of edges per node varies from node to
 432 node, i.e., its edges do not allow us uniformly sample the graph, but they
 433 preferentially lead to high degree nodes [36]. This means that a landscape
 434 with few nodes and a high degree enables that a search at a given node chosen
 435 at random presents more chances to move to one of these high degree nodes
 436 instead to another node, which can efficiently search the entire network.

437 To summarize our analyzes of degree distributions, as most instances
 438 cannot be represented with the straightforward interpretation from power-
 439 law models, another way to analyze the difficulty of the search space for the
 440 heuristics is to consider the size of the basins of attraction – which we will

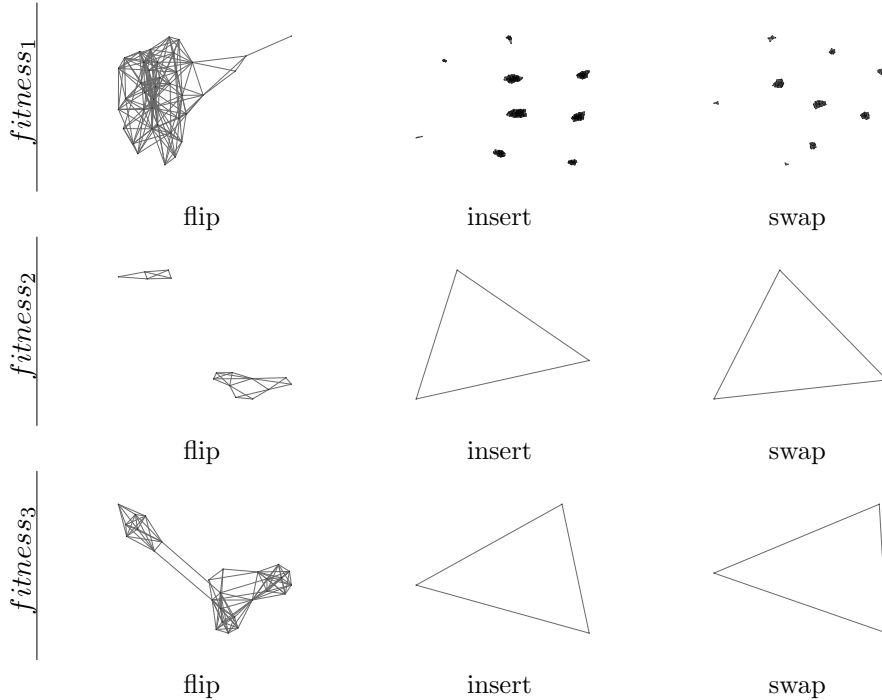


Figure 6: LON graphs for *lex* initialization on $n = 6$ with fitness functions $fitness_1$, $fitness_2$ and $fitness_3$ using 1000 samples for all three operators: flip, insert, swap.

441 explore next.

442 6.3. Basin Size Correlation

443 Our “matrices of plots” present the basin correlation in the middle and
 444 right columns, i.e., Figure 8 and Figure 9 show this for $n = 4$, and Fig-
 445 ures 10, 11, and 12 show these for the larger values of n . A particular focus
 446 of the last three mentioned figures is the difference of 1000 samples to 10000
 447 samples.

448 Let us again start with $n = 4$ in Figures 8 and 9. Firstly, flips and swaps
 449 seem to result in almost perfectly identical LONs. This is interesting, as the
 450 flips generate neighbors with the same Hamming distance to the original,
 451 and swaps generate neighbors with the Hamming distances 0 or 2.

452 Secondly, the swapinsert (green) neighborhood typically results in very
 453 different LONs, as we have already seen in the earlier tables: the local op-
 454 tima are significantly less interconnected. This might result from using two
 455 operators that result in neighbors with the Hamming distance 0 or 2 in com-
 456 bination with the lexicographic sampling. Also, it appears that the use of the
 457 flip operator results in significantly greater basins of attraction – however, as

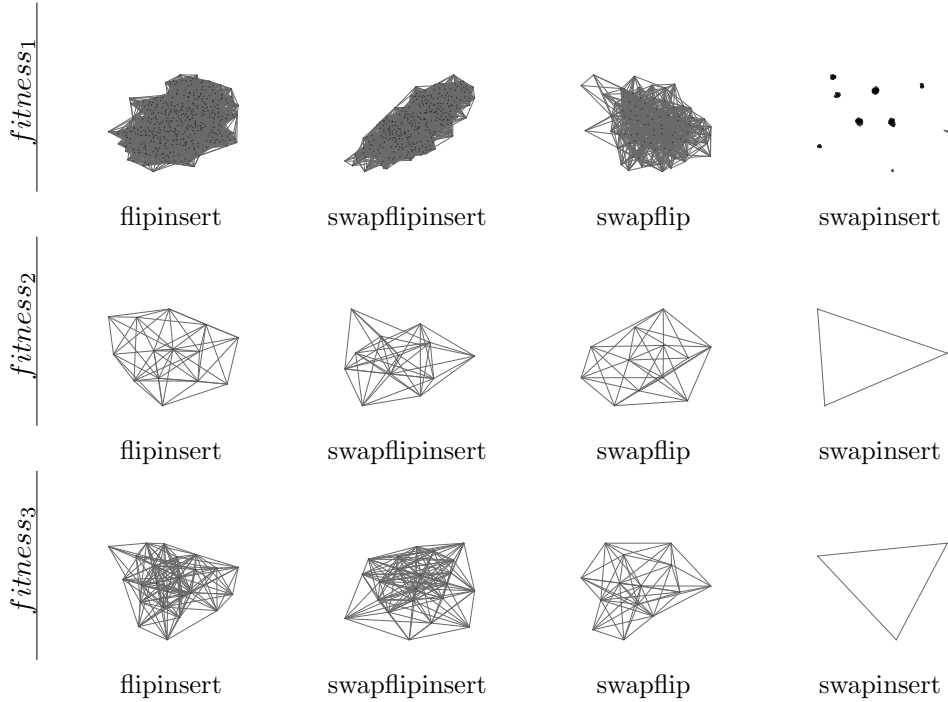


Figure 7: LON graphs for *lex* initialization on $n = 6$ with fitness functions $fitness_1$, $fitness_2$ and $fitness_3$ using 1000 samples for combination using operators flipinsert, swapflipinsert, swapflip, and swapinsert.

458 we are using the lexicographic sampling of the initial solutions, this comes
 459 to no big surprise.

460 Thirdly, we can observe that the three different fitness functions resulted
 461 in quite different landscapes, and in particular, $fitness_1$ is quite different
 462 from the other two. We can see some correlations for $fitness_1$ of basin size
 463 with degree and fitness. At first sight, it is not clear how this information can
 464 be used in a heuristic. However, if techniques like self-adaptation and restarts
 465 are used in combination with $fitness_1$, then the progress achieved over time
 466 can be used in online control to indicate the expected achievable solution
 467 quality. Moreover, it should be possible to estimate this characteristic in a
 468 search heuristic with restarts to influence the amount of perturbation that is
 469 performed on the current best solution (i.e., to provide the first solution for
 470 the next hill-climb): if a solution resulted after a local search presents poor
 471 fitness, then a not-too-small perturbation should be applied to determine the
 472 initial point for the next run, aiming to increase chances to escape the small,
 473 bad basin of attraction. Note that the opposite does not hold, meaning that
 474 a large perturbation does not guarantee success. For $fitness_2$ and $fitness_3$,

475 however, the correlation is a lot weaker and hence might be difficult to exploit.

476 Lastly, let us highlight a few interesting aspects of the landscapes when
477 n is larger, i.e., in Figures 10, 11, and 12. For example, we can observe
478 (except in the case of $n = 6$) that the distance from the black distributions
479 to the blue ones (factor 10 increase in samples) is roughly the same across
480 all experiments — in particular, this applies (roughly) to both dimensions
481 in all three figures. If the increase would be limited to a shift in the y-axis,
482 then this would mean that the 10-fold increase in samples does not uncover
483 different structures (as expressed in different degree distributions) in the
484 landscape. However, the increase along the x-axis means that the rate of
485 uncovering new structures is relatively stable. We believe that the number
486 of samples has yet to be further increased as the degree distributions do not
487 show signs of convergence yet. $n = 6$ with swaps or inserts shows significantly
488 different behavior, and it might be the case that substructures have not been
489 discovered during a local search that resulted in interconnections between
490 the local optima. This warrants additional future research.

491 Besides this, we can generally observe good correlations of degrees and
492 basin sizes when inserts or swaps are used for $n = 5$ and $n = 6$. We can
493 also observe that for $n = 7$ only inserts seem to provide a decent correlation
494 of degrees and basin sizes that might be exploitable, as mentioned above.
495 Also, as before, the fitness of local optima seems to only carry some possibly
496 exploitable information in the case of flips.

497 These experimental results can summarize some insights regarding the
498 search improvements. The topological properties for *fitness*₂ and *fitness*₃
499 are LON of only one component for almost all instances, presenting high
500 mean degree and small minimum distances between nodes. Besides, the lo-
501 cal optima are connected as dense local clusters and sparse interconnections,
502 which can be difficult to exploit. Some heuristics such as Tabu Search with
503 restarts or a Memetic Algorithm with built-in local searches, or even an
504 approach with explicit niching might be able to explore the entire network
505 searching for promising solutions. According to the basin distribution there
506 are few nodes with a large number of neighbors connecting the entire land-
507 scape: a search at a random node has more chances to move to one of these
508 high degree nodes, and then to another node, which can be an efficient way
509 to search the entire network. Moreover flip operator seems to provide more
510 information using basin size and fitness of local optima correlation than the
511 others operators.

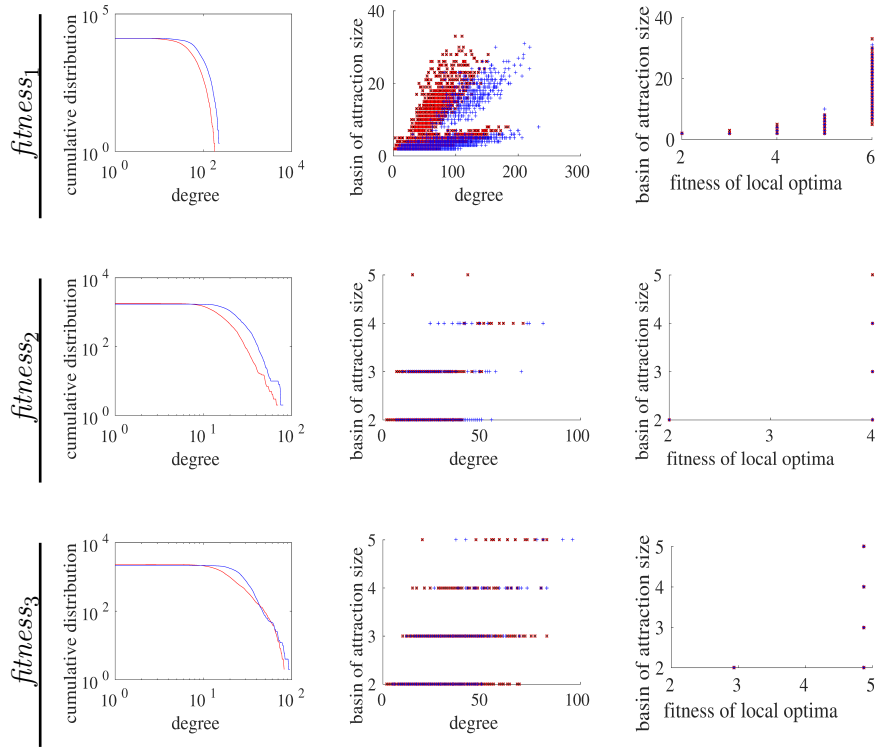


Figure 8: Statistical measures on exhaustive $n = 4$ with the three fitness functions for operators flip (black), insert (blue), swap (red): Cumulative degree distribution in a log-log scale (left), Correlation between the degree of local optima and their corresponding basin sizes (middle), and Correlation between the fitness of local optima and their corresponding basin sizes (right).

512 7. Conclusions

513 Boolean functions are interesting mathematical objects that are widely
 514 used in many domains. Heuristics play an important role in their construc-
 515 tion. However, little is known about the actual problem difficulty and the
 516 effect of various design decisions. This paper conducted a fitness landscape
 517 analysis (FLA) to study the effect of various decisions on the optimization
 518 of cryptographic properties. We investigated Boolean functions considering a
 519 different number of function sizes, three fitness functions, seven neighborhood
 520 operators used in isolation as well as in combination, and two initialization
 521 strategies.

522 We presented and analyzed the local optima networks (LONs) obtained

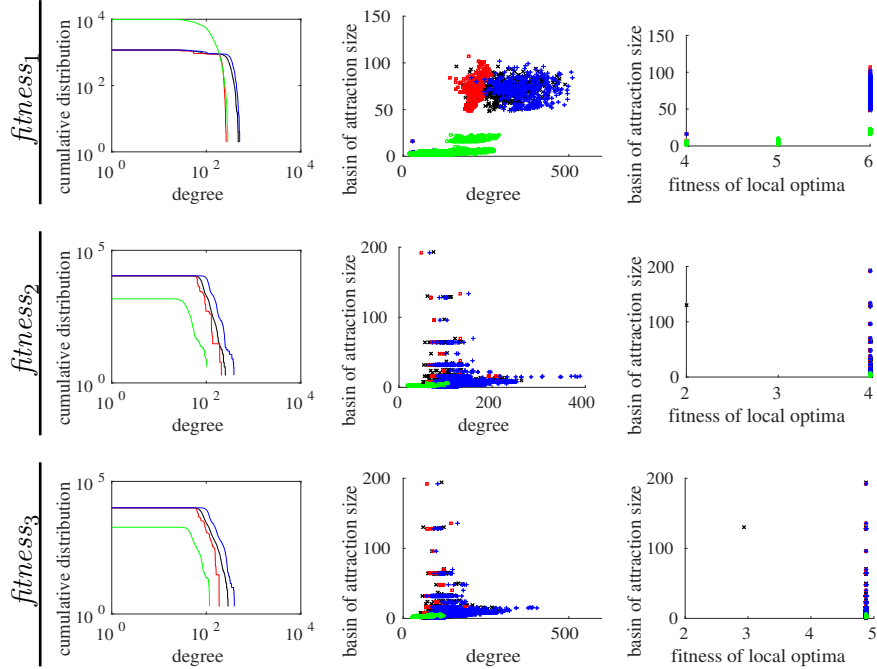


Figure 9: Statistical measures on exhaustive $n = 4$ with the three fitness functions for combination using operators flipinsert (black), swapflipinsert (blue), swapflip (red), and swapinsert (green): Cumulative degree distribution in a log-log scale (left), Correlation between the degree of local optima and their corresponding basin sizes (middle), and Correlation between the fitness of local optima and their corresponding basin sizes (right).

523 using a local search heuristic to investigate the search space structure. Fur-
 524 thermore, we studied the degree distribution and the correlation between the
 525 basins of attraction with some LON properties looking for additional infor-
 526 mation about the search difficulty, considering scenarios (e.g., combinations
 527 of neighborhoods) not investigated before.

528 We have observed (1) that the naive fitness function results in LONs with
 529 disconnected components, (2) which can typically be avoided by moving to
 530 other fitness functions. However, (3) we then appear to lose a correlation
 531 of basin size and LON degrees. (4) For our largest $n = 7$ (i.e., when the
 532 search space is 2^{128}), inserts appear to provide the largest possible exploitable
 533 correlation of basin sizes, local optima degrees, and local optima fitness.

534 In this paper, we concentrated on Boolean functions with 4 to 7 variables.
 535 In future work, we plan to extend our analysis up to 10 variables (i.e., up

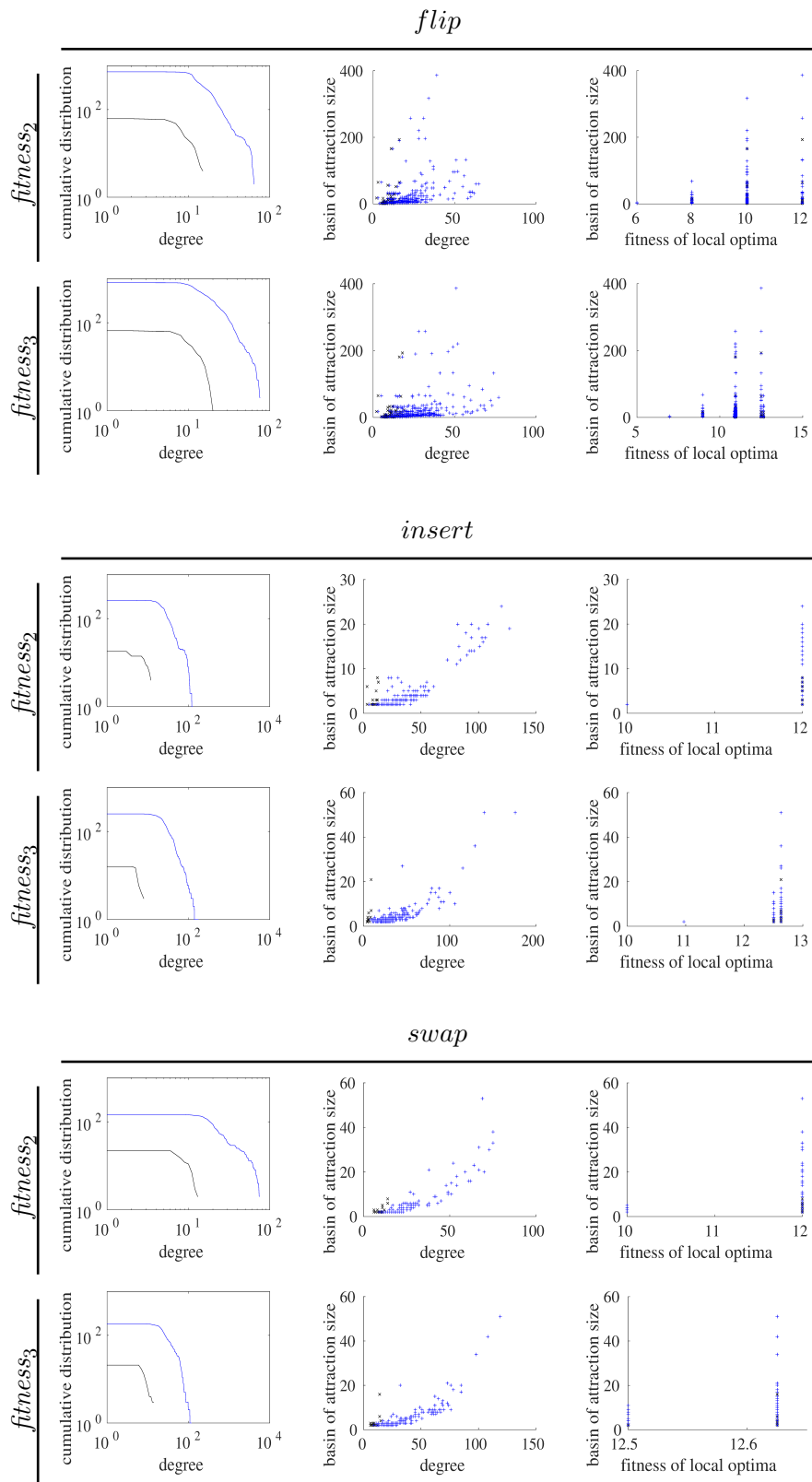


Figure 10: Statistical measures for *lex* initialization on $n = 5$ with fitness functions *fitness₂* and *fitness₃* using 1000 (black) and 10000 (blue) samples for all three operators: Cumulative degree distribution in a log-log scale (left), Correlation between the degree of local optima and their corresponding basin sizes (middle), and Correlation between the fitness of local optima and their corresponding basin sizes (right).

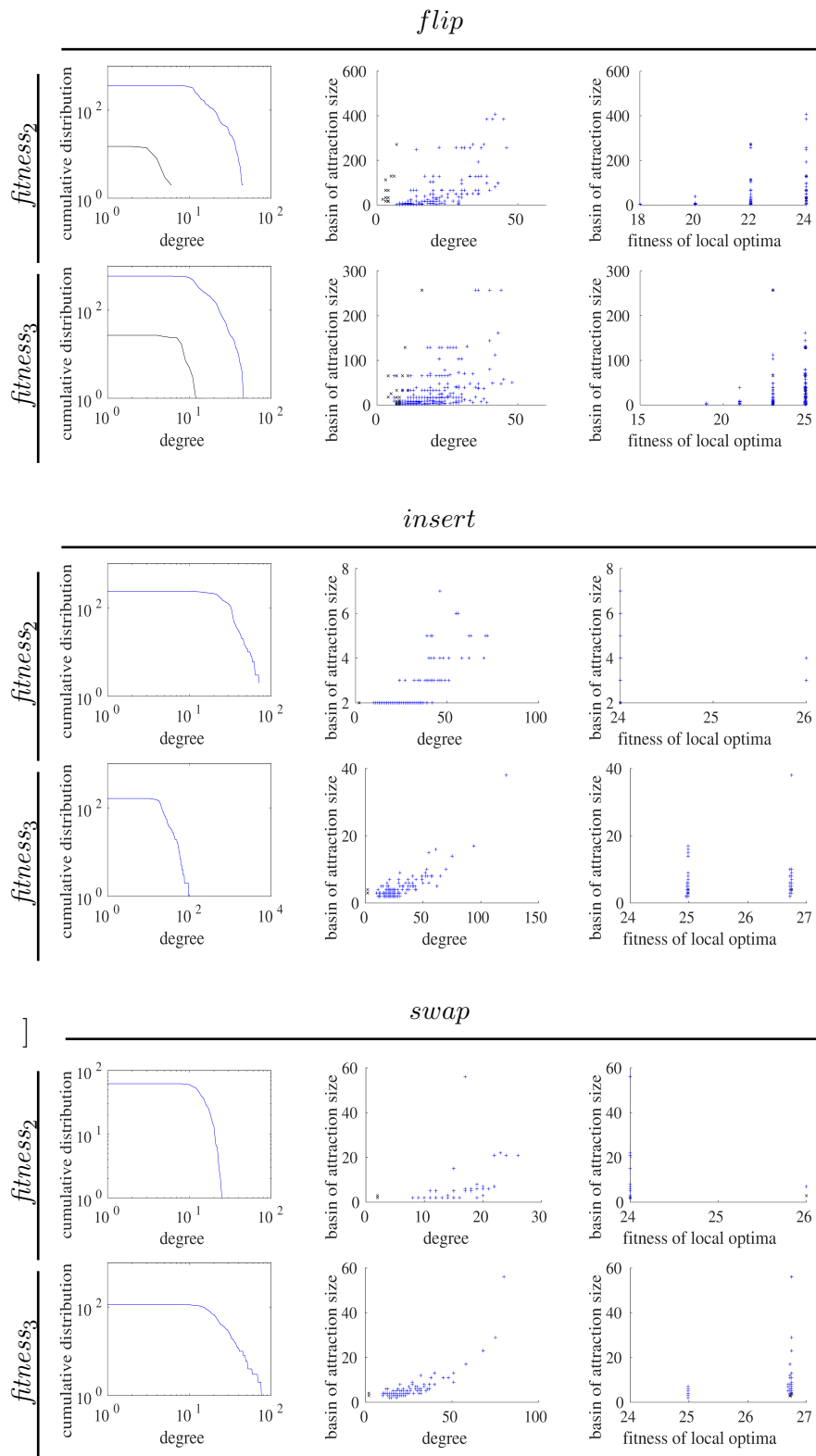
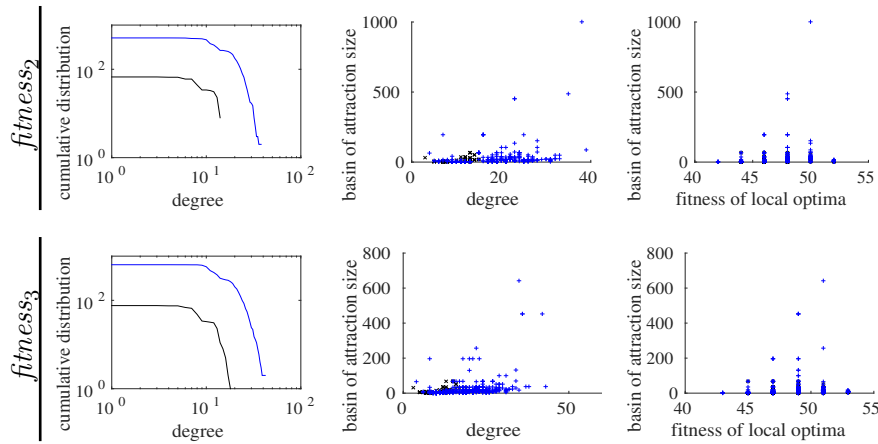
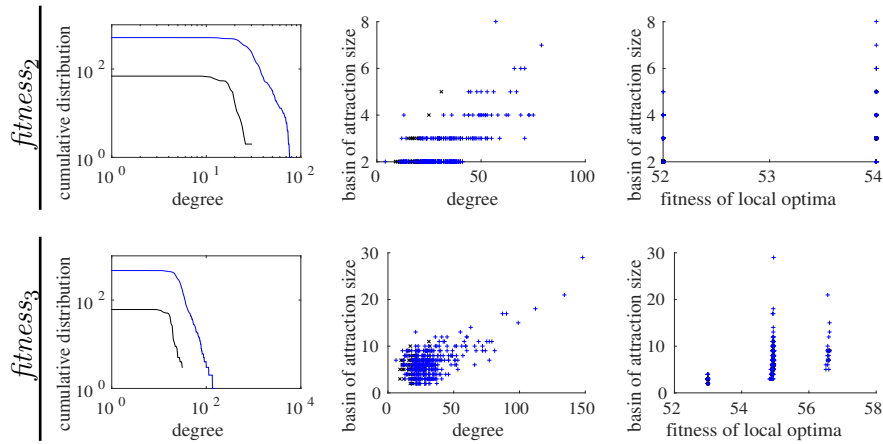


Figure 11: Statistical measures for *lex* initialization on $n = 6$ with fitness functions *fitness₂* and *fitness₃* using 1000 (black) and 10000 (blue) samples for all three operators: Cumulative degree distribution in a log-log scale (left), Correlation between the degree of local optima and their corresponding basin sizes (middle), and Correlation between the fitness of local optima and their corresponding basin sizes (right). Note that, in a few cases in the left column, no black line can be drawn as not enough points exist for a log-log plot.

flip



insert



swap

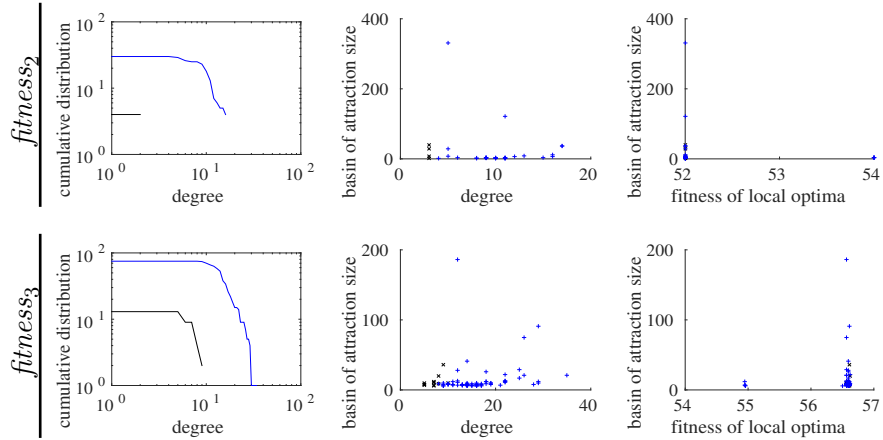


Figure 12: Statistical measures for *lex* initialization on $n = 7$ with fitness functions $fitness_2$ and $fitness_3$ using 1000 (black) and 10000 (blue) samples for all three operators: Cumulative degree distribution in a log-log scale (left), Correlation between the degree of local optima and their corresponding basin sizes (middle), and Correlation between the fitness of local optima and their corresponding basin sizes (right).

536 to 1 024 bits), which will require new approaches for evaluating complete
537 neighborhoods.

538 **Acknowledgements**

539 Our work was supported by the Australian Research Council projects
540 DE160100850, DP200102364, and DP210102670. Parts of our work have been
541 inspired by COST Action CA15140 supported by COST (European Cooper-
542 ation in Science and Technology).

543 **References**

- 544 [1] O. Rothaus, On “bent” functions, *Journal of Combinatorial Theory,*
545 *Series A* 20 (3) (1976) 300 – 305.
- 546 [2] A. Bernasconi, B. Codenotti, J. M. Vanderkam, A characterization of
547 bent functions in terms of strongly regular graphs, *IEEE Transactions*
548 *on Computers* 50 (9) (2001) 984–985.
- 549 [3] X. Huang, K. Fang, L. Fang, Q. Chen, Z.-R. Lai, L. Wei, Bi-
550 kronecker functional decision diagrams: A novel canonical representa-
551 tion of boolean functions, in: *AAAI Conference on Artificial Intelligence,*
552 *Vol. 33, 2019,* pp. 2867–2875.
- 553 [4] S. Kavut, S. Maitra, M. D. Yucel, Search for boolean functions with
554 excellent profiles in the rotation symmetric class, *IEEE Transactions on*
555 *Information Theory* 53 (5) (2007) 1743–1751.
- 556 [5] A. Kerdock, A class of low-rate nonlinear binary codes, *Information and*
557 *Control* 20 (2) (1972) 182 – 187.
- 558 [6] J. Olsen, R. Scholtz, L. Welch, Bent-function sequences, *IEEE Trans.*
559 *on Information Theory* 28 (6) (1982) 858–864.
- 560 [7] K. Paterson, On Codes With Low Peak-to-Average Power Ratio for
561 Multicode CDMA, *IEEE Transactions on Information Theory* 50 (2004)
562 550 – 559.
- 563 [8] M. Hell, T. Johansson, A. Maximov, W. Meier, A stream cipher pro-
564 posal: Grain-128, in: *IEEE Int. Symposium on Information Theory, 2006,*
565 *pp. 1614–1618.*
- 566 [9] C. M. Adams, Constructing symmetric ciphers using the cast design
567 procedure, *Designs, Codes and Cryptography* 12 (3) (1997) 283–316.
- 568 [10] Y. Zheng, J. Pieprzyk, J. Seberry, HAVAL — a one-way hashing algo-
569 rithm with variable length of output (extended abstract), in: *Advances*
570 *in Cryptology — AUSCRYPT ’92: Workshop on the Theory and Appli-*
571 *cation of Cryptographic Techniques, Springer, 1993,* pp. 81–104.

- 572 [11] S. Picek, D. Sisejkovic, V. Rozic, B. Yang, D. Jakobovic, N. Mentens,
573 Evolving cryptographic pseudorandom number generators, in: *Parallel*
574 *Problem Solving from Nature (PPSN)*, Springer, 2016, pp. 613–622.
- 575 [12] S. Picek, D. Jakobovic, J. F. Miller, E. Marchiori, L. Batina, Evolutionary
576 Methods for the Construction of Cryptographic Boolean Functions,
577 in: *18th European Conference on Genetic Programming (EuroGP)*, 2015,
578 pp. 192–204.
- 579 [13] S. Picek, C. Carlet, S. Guilley, J. F. Miller, D. Jakobovic, Evolutionary
580 algorithms for boolean functions in diverse domains of
581 cryptography, *Evolutionary Computation* 24 (4) (2016) 667–694.
582 doi:10.1162/EVCO_a_00190.
583 URL https://doi.org/10.1162/EVCO_a_00190
- 584 [14] L. Mariot, S. Picek, D. Jakobovic, A. Leporati, Evolutionary search of
585 binary orthogonal arrays, in: *Parallel Problem Solving from Nature –*
586 *PPSN XV*, Springer, 2018, pp. 121–133.
- 587 [15] L. Mariot, S. Picek, D. Jakobovic, A. Leporati, Evolutionary algorithms
588 for the design of orthogonal latin squares based on cellular automata, in:
589 *Genetic and Evolutionary Computation Conference (GECCO)*, ACM,
590 2017, pp. 306–313.
- 591 [16] G. Ochoa, S. Verel, F. Daolio, M. Tomassini, Local optima networks: A
592 new model of combinatorial fitness landscapes, in: *Recent Advances in*
593 *the Theory and Application of Fitness Landscapes*, Springer, 2014, pp.
594 233–262.
- 595 [17] C. Carlet, Boolean functions for cryptography and error correcting
596 codes, *Boolean models and methods in mathematics, computer science,*
597 *and engineering* 2 (2010) 257–397.
- 598 [18] J. Dillon, A Survey of Bent Functions*, Tech. rep., Reprinted from the
599 NSA Technical Journal. Special Issue, unclassified (1972).
- 600 [19] W. Millan, A. Clark, E. Dawson, An Effective Genetic Algorithm for
601 Finding Highly Nonlinear Boolean Functions, in: *First Int. Conference*
602 *on Information and Communication Security, ICICS '97*, Springer, 1997,
603 pp. 149–158.

- 604 [20] W. Millan, A. Clark, E. Dawson, Heuristic design of cryptographically
605 strong balanced Boolean functions, in: *Advances in Cryptology - EU-*
606 *ROCRYPT '98*, 1998, pp. 489–499.
- 607 [21] J. A. Clark, J. L. Jacob, Two-Stage Optimisation in the Design of
608 Boolean Functions, in: *Information Security and Privacy*, Vol. 1841 of
609 LNCS, Springer, 2000, pp. 242–254.
- 610 [22] S. Kavut, M. D. Yücel, Improved Cost Function in the Design of Boolean
611 Functions Satisfying Multiple Criteria, in: *Progress in Cryptology - IN-*
612 *DOCRYPT 2003*, Vol. 2904 of LNCS, Springer, 2003, pp. 121–134.
- 613 [23] W. Millan, J. Fuller, E. Dawson, New concepts in evolutionary search
614 for Boolean functions in cryptology, *Computational Intelligence* 20 (3)
615 (2004) 463–474.
- 616 [24] H. Aguirre, H. Okazaki, Y. Fuwa, An Evolutionary Multiobjective Ap-
617 proach to Design Highly Non-linear Boolean Functions, in: *Genetic and*
618 *Evolutionary Computation Conference (GECCO)*, 2007, pp. 749–756.
- 619 [25] S. Picek, D. Jakobovic, M. Golub, Evolving Cryptographically Sound
620 Boolean Functions, in: *Genetic and Evolutionary Computation Confer-*
621 *ence (GECCO)*, *GECCO '13 Companion*, ACM, 2013, pp. 191–192.
- 622 [26] S. Picek, R. I. McKay, R. Santana, T. Gedeon, Fighting the symmetries:
623 The structure of cryptographic boolean function spaces, in: *Genetic and*
624 *Evolutionary Computation Conference, GECCO*, ACM, 2015, pp. 457–
625 464. doi:10.1145/2739480.2754739.
626 URL <http://dl.acm.org/citation.cfm?id=2739480>
- 627 [27] L. Mariot, A. Leporati, Heuristic Search by Particle Swarm Optimization
628 of Boolean Functions for Cryptographic Applications, in: *Genetic and*
629 *Evolutionary Computation Conference, GECCO*, *Companion Material*
630 *Proceedings*, 2015, pp. 1425–1426.
- 631 [28] S. Picek, D. Jakobovic, J. F. Miller, L. Batina, M. Cupic, Cryptographic
632 Boolean functions: One output, many design criteria, *Appl. Soft Com-*
633 *put.* 40 (2016) 635–653.

- 634 [29] S. Picek, D. Sisejkovic, D. Jakobovic, Immunological algorithms
635 paradigm for construction of boolean functions with good cryptographic
636 properties, *Eng. Appl. of AI* 62 (2017) 320–330.
- 637 [30] R. Hrbacek, V. Dvorak, Bent Function Synthesis by Means of Cartesian
638 Genetic Programming, in: *Parallel Problem Solving from Nature - PPSN*
639 *XIII*, Vol. 8672 of LNCS, Springer, 2014, pp. 414–423.
- 640 [31] S. Picek, D. Jakobovic, Evolving Algebraic Constructions for Designing
641 Bent Boolean Functions, 2016, pp. 781–788.
- 642 [32] K. Knezevic, S. Picek, L. Mariot, D. Jakobovic, A. Leporati, The design
643 of (almost) disjunct matrices by evolutionary algorithms, in: *Theory and*
644 *Practice of Natural Computing*, Springer, 2018, pp. 152–163.
- 645 [33] S. Kauffman, S. Levin, Towards a general theory of adaptive walks on
646 rugged landscapes, *Journal of Theoretical Biology* 128 (1) (1987) 11–45.
- 647 [34] G. Ochoa, M. Tomassini, S. Vérel, C. Darabos, A study of NK land-
648 scapes’ basins and local optima networks, in: *Genetic and Evolutionary*
649 *Computation Conference (GECCO)*, ACM, 2008, pp. 555–562.
- 650 [35] S. Vérel, F. Daolio, G. Ochoa, M. Tomassini, Local optima networks
651 with escape edges., in: *Artificial Evolution*, Springer, 2011, pp. 49–60.
- 652 [36] M. E. Yafrani, M. S. R. Martins, M. E. Krari, M. Wagner, M. R. B. S.
653 Delgado, B. Ahiod, R. Lüders, A fitness landscape analysis of the trav-
654 elling thief problem, in: *Genetic and Evolutionary Computation Confer-*
655 *ence (GECCO)*, ACM, 2018, pp. 277–284.
- 656 [37] D. Jakobovic, S. Picek, M. S. Martins, M. Wagner, A characterisation of
657 s-box fitness landscapes in cryptography, in: *Proceedings of the Genetic*
658 *and Evolutionary Computation Conference*, 2019, pp. 285–293.
- 659 [38] M. Tomassini, S. Verel, G. Ochoa, Complex-network analysis of com-
660 binatorial spaces: The NK landscape case, *Physical Review E* 78 (6)
661 (2008) 066114.
- 662 [39] F. Chicano, F. Daolio, G. Ochoa, S. Vérel, M. Tomassini, E. Alba, Local
663 optima networks, landscape autocorrelation and heuristic search perfor-
664 mance, *Parallel Problem Solving from Nature (PPSN)* (2012) 337–347.

- 665 [40] F. Daolio, S. Verel, G. Ochoa, M. Tomassini, Local optima networks and
666 the performance of iterated local search, in: Genetic and Evolutionary
667 Computation Conference, GECCO, ACM, 2012, pp. 369–376.
- 668 [41] F. Daolio, S. Verel, G. Ochoa, M. Tomassini, Local optima networks
669 of the permutation flow-shop problem, in: International Conference on
670 Artificial Evolution (Evolution Artificielle), Springer, 2013, pp. 41–52.
- 671 [42] G. Ochoa, N. Veerapen, F. Daolio, M. Tomassini, Understanding phase
672 transitions with local optima networks: number partitioning as a case
673 study, in: European Conference on Evolutionary Computation in Com-
674 binatorial Optimization, Springer, 2017, pp. 233–248.
- 675 [43] L. Hernando, F. Daolio, N. Veerapen, G. Ochoa, Local optima networks
676 of the permutation flowshop scheduling problem: Makespan vs. total flow
677 time, in: IEEE Congress on Evolutionary Computation (CEC), IEEE,
678 2017, pp. 1964–1971.
- 679 [44] F. Chicano, D. Whitley, G. Ochoa, R. Tinós, Optimizing one million
680 variable NK landscapes by hybridizing deterministic recombination and
681 local search, in: Genetic and Evolutionary Computation Conference
682 (GECCO), ACM, 2017, pp. 753–760.
- 683 [45] F. Glover, Tabu search - Part I, *ORSA Journal on Computing* 1 (3)
684 (1989) 190–206.
- 685 [46] F. Glover, Tabu search - Part II, *ORSA Journal on Computing* 2 (1)
686 (1990) 4–32.
- 687 [47] P. Moscato, *New ideas in optimization*, McGraw-Hill Ltd., UK, 1999,
688 Ch. Memetic Algorithms: A Short Introduction, pp. 219–234.
- 689 [48] L. A. Adamic, R. M. Lukose, B. A. Huberman, Local search in unstruc-
690 tured networks, *Handbook of Graphs and Networks: from the Genome
691 to the Internet* (2006).
- 692 [49] A. Clauset, C. R. Shalizi, M. E. Newman, Power-law distributions in
693 empirical data, *SIAM Review* 51 (4) (2009) 661–703.
- 694 [50] W. Deng, W. Li, X. Cai, Q. A. Wang, The exponential degree distribu-
695 tion in complex networks: Non-equilibrium network theory, numerical

696 simulation and empirical data, Physica A: Statistical Mechanics and its
697 Applications 390 (8) (2011) 1481–1485.

698 **Appendix with Supplemental Material**

699 We make use of the appendix in order to provide additional visualizations of
700 the results. In particular:

- 701 1. $n = 4$: Table .6 shows the metrics when considering the sample process
702 for $n = 4$ for both lex and random initialization with 1 000 and 10 000
703 samples.
- 704 2. $n = 5$: Figure .13 shows the difference between the two initialization
705 strategies, which we had not visualized before. Figure .14 shows the
706 complex neighborhoods for 1 000 samples.
- 707 3. $n = 6$: Figure .15 shows the individual neighborhoods for 1 000 samples.
708 Figure .16 shows the complex neighborhoods for 1 000 samples.
- 709 4. Figures .17-.20 show, for 10 000 samples, the results for the neighbor-
710 hoods in isolation and in combination for $fitness_2$ and $fitness_3$.

Samples	Initialization	Function	Operator	n_v	n_e	z	C	C_r	b	l	π	S		
1 000	lex	$fitness_1$	<i>flip</i>	121	520	8.5950	0.3526	0.0858	9.0000	—	0	2		
			<i>insert</i>	438	3363	15.3562	0.5590	0.0381	2.8607	—	0	13		
			<i>swap</i>	306	1948	12.7320	0.6407	0.0424	4.7516	—	0	14		
			<i>flipinsert</i>	182	2494	27.4066	0.5753	0.1508	6.6374	2.0764	1	1		
			<i>swapflip</i>	306	3514	22.9673	0.4806	0.0763	4.7516	3.0680	1	1		
			<i>swapflipinsert</i>	363	5279	29.0854	0.4869	0.0807	4.3140	2.9272	1	1		
		$fitness_2$	<i>swapinsert</i>	363	3325	18.3196	0.6810	0.0492	4.3140	—	0	11		
			<i>flip</i>	185	849	9.1784	0.3165	0.0494	5.2973	—	0	2		
			<i>insert</i>	626	5660	18.0831	0.4115	0.0297	2.0272	—	0	11		
			<i>swap</i>	379	2236	11.7995	0.5123	0.0292	4.3140	—	0	20		
			<i>flipinsert</i>	185	2132	23.0486	0.4563	0.1244	5.4216	—	0	2		
			<i>swapflip</i>	379	3416	18.0264	0.4235	0.0458	4.3140	—	0	2		
		$fitness_3$	<i>swapflipinsert</i>	382	4208	22.0314	0.4484	0.0578	4.2749	—	0	2		
			<i>swapinsert</i>	382	3005	15.7330	0.5823	0.0392	4.2749	—	0	19		
			<i>flip</i>	173	802	9.2717	0.3259	0.0588	5.5954	—	0	2		
			<i>insert</i>	630	5630	17.8730	0.4157	0.0301	2.0397	—	0	9		
			<i>swap</i>	387	2334	12.0620	0.5106	0.0333	4.2765	—	0	19		
			<i>flipinsert</i>	173	2054	23.7457	0.4820	0.1400	5.7977	—	0	2		
		1 000	random	$fitness_1$	<i>swapflip</i>	387	3650	18.8630	0.4224	0.0459	4.2765	—	0	2
					<i>swapflipinsert</i>	390	4470	22.9231	0.4484	0.0600	4.2385	—	0	2
					<i>swapinsert</i>	390	3131	16.0564	0.5924	0.0409	4.2385	—	0	19
					<i>flip</i>	972	1	0.0021	0.0000	0.0000	3.1173	—	0	971
					<i>insert</i>	835	0	0.0000	0.0000	0.0000	2.1449	—	0	835
					<i>swap</i>	972	1	0.0021	0.0000	0.0000	2.6173	—	0	971
				$fitness_2$	<i>flipinsert</i>	987	0	0.0000	0.0000	0.0000	2.5502	—	0	987
					<i>swapflip</i>	972	1	0.0021	0.0000	0.0000	2.6173	—	0	971
					<i>swapflipinsert</i>	987	3	0.0061	0.0000	0.0000	2.5380	—	0	984
					<i>swapinsert</i>	987	2	0.0041	0.0000	0.0000	2.5380	—	0	985
					<i>flip</i>	803	0	0.0000	0.0000	0.0000	2.9178	—	0	803
					<i>insert</i>	692	0	0.0000	0.0000	0.0000	2.2934	—	0	692
				$fitness_3$	<i>swap</i>	832	6	0.0144	0.0000	0.0000	2.9075	—	0	826
					<i>flipinsert</i>	832	0	0.0000	0.0000	0.0000	2.9014	—	0	832
					<i>swapflip</i>	832	8	0.0192	0.0000	0.0000	2.9123	—	0	824
					<i>swapflipinsert</i>	832	10	0.0240	0.0000	0.0000	2.9038	—	0	822
					<i>swapinsert</i>	832	8	0.0192	0.0000	0.0000	2.8990	—	0	824
					<i>flip</i>	803	0	0.0000	0.0000	0.0000	2.9178	—	0	803
10 000	lex			$fitness_1$	<i>insert</i>	704	0	0.0000	0.0000	0.0000	2.2884	—	0	704
					<i>swap</i>	844	6	0.0142	0.0000	0.0000	2.8945	—	0	838
					<i>flipinsert</i>	844	0	0.0000	0.0000	0.0000	2.8886	—	0	844
					<i>swapflip</i>	844	8	0.0190	0.0000	0.0000	2.8993	—	0	836
					<i>swapflipinsert</i>	844	12	0.0284	0.0000	0.0000	2.8910	—	0	832
					<i>swapinsert</i>	844	10	0.0237	0.0000	0.0000	2.8863	—	0	834
				$fitness_2$	<i>flip</i>	732	6286	17.1749	0.3105	0.0233	14.2514	2.9103	1	1
					<i>insert</i>	3574	71540	40.0336	0.3816	0.0113	3.3898	—	0	11
					<i>swap</i>	1785	32130	36.0000	0.4864	0.0199	7.3647	—	0	14
					<i>flipinsert</i>	938	37871	80.7484	0.4886	0.0855	11.9872	2.1088	1	1
					<i>swapflip</i>	1785	52112	58.3888	0.3814	0.0326	7.3647	3.1423	1	1
					<i>swapflipinsert</i>	2035	88221	86.7037	0.3988	0.0429	6.8590	3.0030	1	1
$fitness_3$	<i>swapinsert</i>			2035	62664	61.5862	0.5420	0.0302	6.8590	—	0	14		
	<i>flip</i>			1835	13696	14.9275	0.2121	0.0085	5.3232	—	0	2		
	<i>insert</i>			5289	99516	37.6313	0.2836	0.0072	2.1624	—	0	8		
	<i>swap</i>			3797	56380	29.6971	0.3364	0.0078	4.3303	—	0	14		
	<i>flipinsert</i>			1812	48743	53.8002	0.2743	0.0299	5.5425	2.9435	1	1		
	<i>swapflip</i>			3796	75460	39.7576	0.2920	0.0105	4.3314	4.2448	1	1		
10 000	random	$fitness_1$	<i>swapflipinsert</i>	3840	107445	55.9609	0.2797	0.0147	4.2745	3.8454	1	1		
			<i>swapinsert</i>	3841	87823	45.7292	0.3417	0.0118	4.2734	—	0	14		
			<i>flip</i>	1707	13253	15.5278	0.2230	0.0082	5.6473	—	0	2		
			<i>insert</i>	5281	99007	37.4956	0.2841	0.0070	2.1888	—	0	9		
			<i>swap</i>	3777	58117	30.7742	0.3377	0.0079	4.3818	—	0	14		
			<i>flipinsert</i>	1683	47481	56.4242	0.2861	0.0336	5.9673	2.8311	1	1		
		$fitness_2$	<i>swapflip</i>	3776	78943	41.8130	0.2926	0.0110	4.3829	4.1114	1	1		
			<i>swapflipinsert</i>	3819	111198	58.2341	0.2819	0.0153	4.3263	3.7668	1	1		
			<i>swapinsert</i>	3820	89878	47.0565	0.3470	0.0123	4.3251	—	0	14		
			<i>flip</i>	9698	11	0.0023	0.0000	0.0000	3.1448	—	0	9687		
			<i>insert</i>	8335	29	0.0070	0.0000	0.0000	2.1445	—	0	8306		
			<i>swap</i>	9698	93	0.0192	0.0003	0.0000	2.6172	—	0	9606		
10 000	random	$fitness_1$	<i>flipinsert</i>	9831	88	0.0179	0.0000	0.0000	2.5442	—	0	9743		
			<i>swapflip</i>	9697	130	0.0268	0.0005	0.0000	2.6176	—	0	9569		
			<i>swapflipinsert</i>	9828	194	0.0395	0.0002	0.0000	2.5308	—	0	9635		
			<i>swapinsert</i>	9829	153	0.0311	0.0000	0.0000	2.5305	—	0	9676		
			<i>flip</i>	8033	5	0.0012	0.0000	0.0000	2.9512	—	0	8028		
			<i>insert</i>	6848	28	0.0082	0.0000	0.0000	2.3112	—	0	6820		
		$fitness_2$	<i>swap</i>	8332	534	0.1282	0.0061	0.0000	2.9399	—	0	7881		
			<i>flipinsert</i>	8353	43	0.0103	0.0000	0.0000	2.9251	—	0	8310		
			<i>swapflip</i>	8326	744	0.1787	0.0084	0.0000	2.9455	—	0	7774		
			<i>swapflipinsert</i>	8325	1108	0.2662	0.0115	0.0000	2.9348	—	0	7559		
			<i>swapinsert</i>	8331	881	0.2115	0.0108	0.0000	2.9292	—	0	7648		
			<i>flip</i>	8033	4	0.0010	0.0000	0.0000	2.9512	—	0	8029		
$fitness_3$	<i>insert</i>	6963	29	0.0083	0.0000	0.0000	2.3078	—	0	6934				
	<i>swap</i>	8445	505	0.1196	0.0065	0.0000	2.9275	—	0	8010				
	<i>flipinsert</i>	8468	40	0.0094	0.0000	0.0000	2.9127	—	0	8428				
	<i>swapflip</i>	8438	690	0.1635	0.0082	0.0000	2.9333	—	0	7899				
	<i>swapflipinsert</i>	8437	1058	0.2508	0.0102	0.0000	2.9230	—	0	7679				
	<i>swapinsert</i>	8444	853	0.2020	0.0097	0.0000	2.9172	—	0	7769				

Table .6: General LON and basins' statistics for $n = 4$ with 1 000 and 10 000 samples, considering lex and random initialization. A dash is shown when l cannot be computed as multiple disconnected components exist.

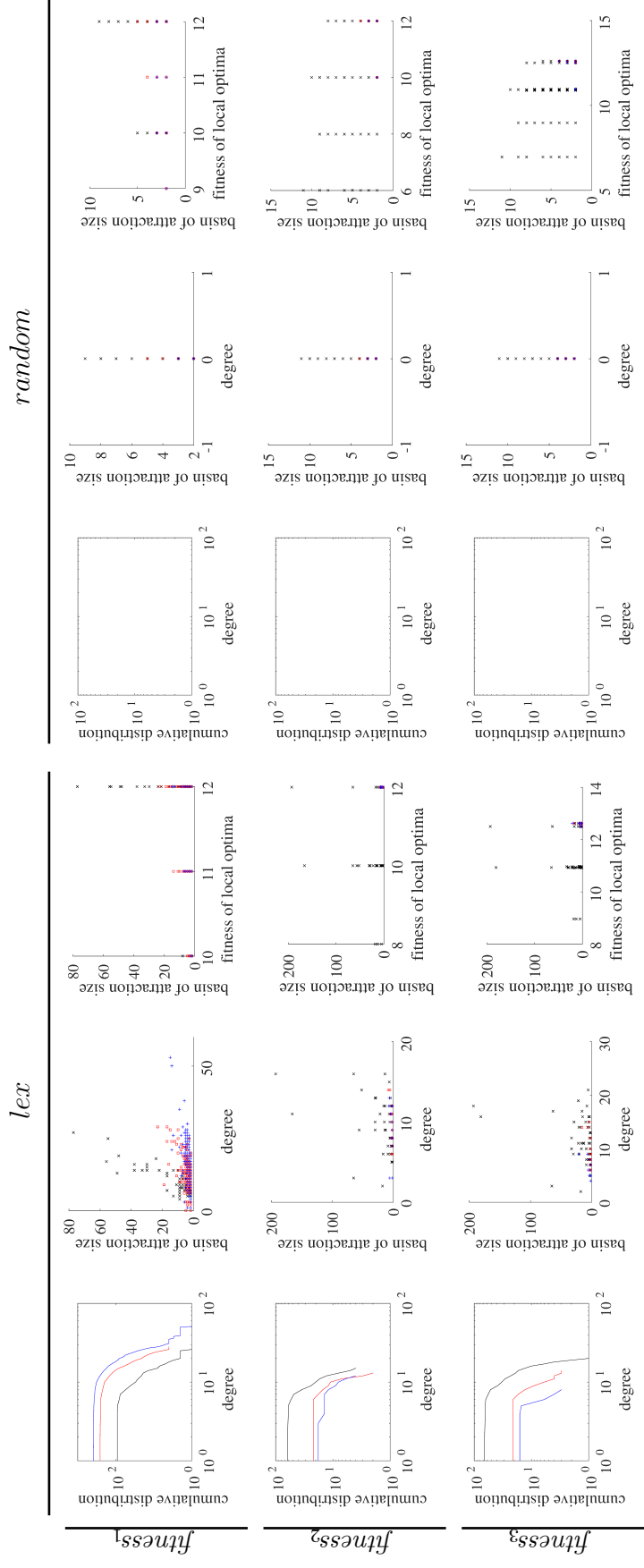


Figure .13: Statistical measures for *lex* (left) and *random* (right) initialization on $n = 5$ with the three fitness functions for operators flip (black), insert (blue), swap (red) using 1 000 samples (within each block of three): Cumulative degree distribution in a log-log scale (left), Correlation between the degree of local optima and their corresponding basin sizes (middle), and Correlation between the fitness of local optima and corresponding basin sizes (right). The forth column is blank, as nodes are of degree 0 ($z = 0$) (see fifth column).

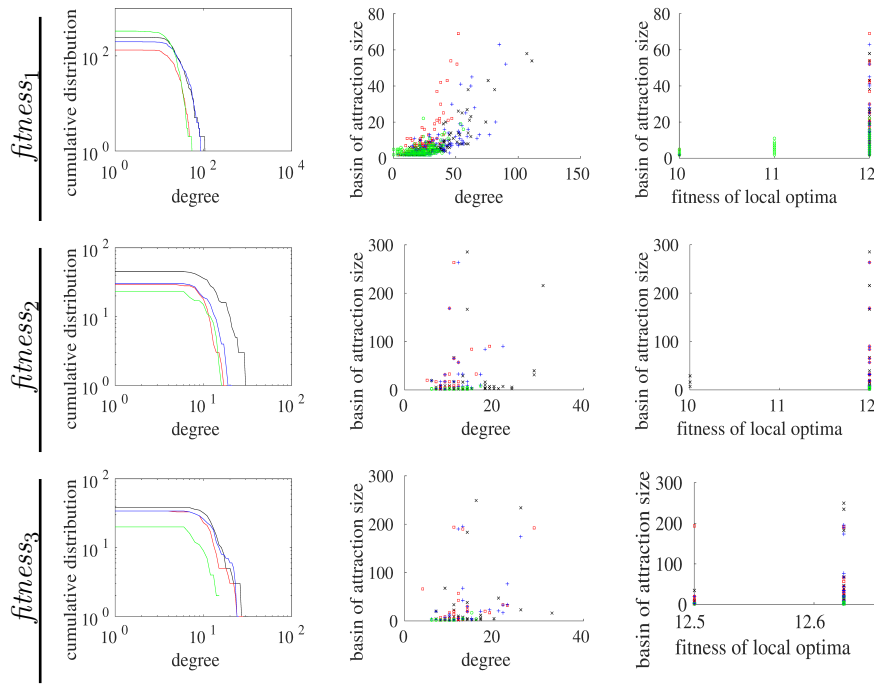


Figure .14: Statistical measures for *lex* initialization on $n = 5$ with the three fitness functions for combination using operators flipinsert (black), swapflipinsert (blue), swapflip (red), and swapinsert (green) using 1000 samples: Cumulative degree distribution in a log-log scale (left), Correlation between the degree of local optima and their corresponding basin sizes (middle), and Correlation between the fitness of local optima and corresponding basin sizes (right).

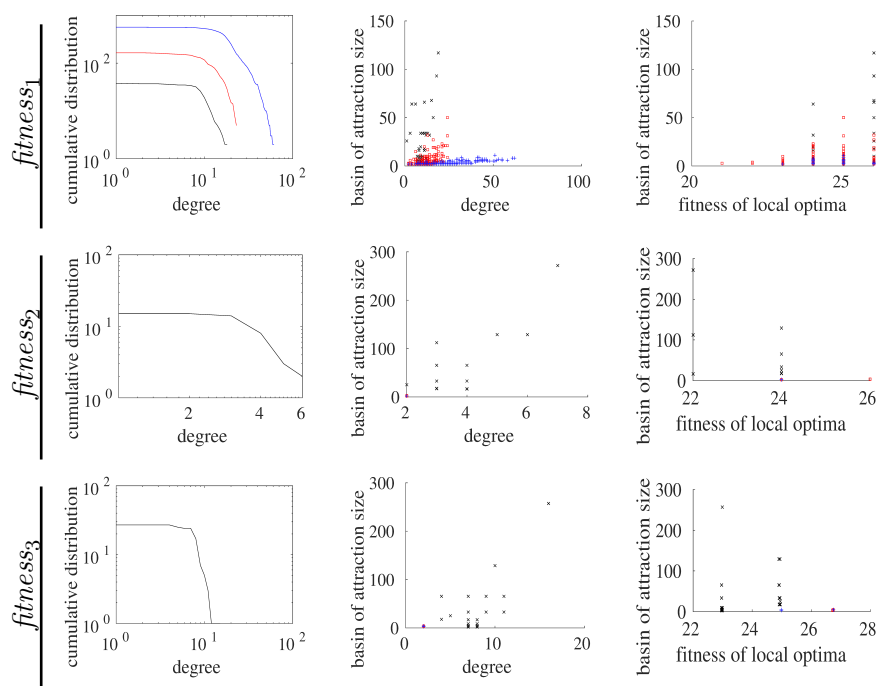


Figure .15: Statistical measures for *lex* initialization on $n = 6$ with the three fitness functions for operators flip (black), insert (blue), swap (red) using 1 000 samples: Cumulative degree distribution in a log-log scale (left), Correlation between the degree of local optima and their corresponding basin sizes (middle), and Correlation between the fitness of local optima and corresponding basin sizes (right).

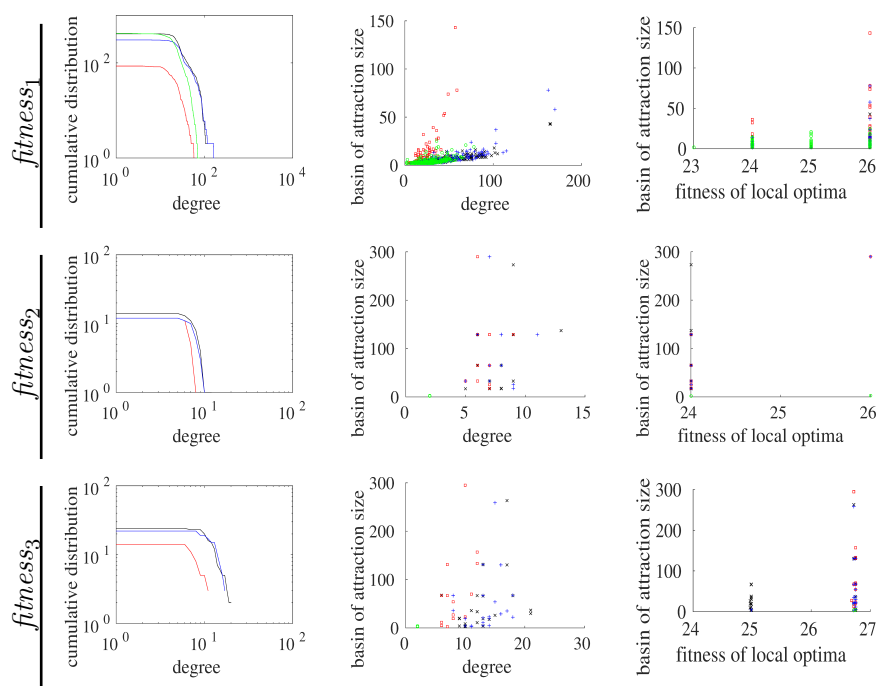


Figure .16: Statistical measures for *lex* initialization on $n = 6$ with fitness functions $fitness_2$ and $fitness_3$ for combination using operators flipinsert (black), swapflipinsert (blue), swapflip (red), and swapinsert (green) using 1000 samples: Cumulative degree distribution in a log-log scale (left), Correlation between the degree of local optima and their corresponding basin sizes (middle), and Correlation between the fitness of local optima and corresponding basin sizes (right).

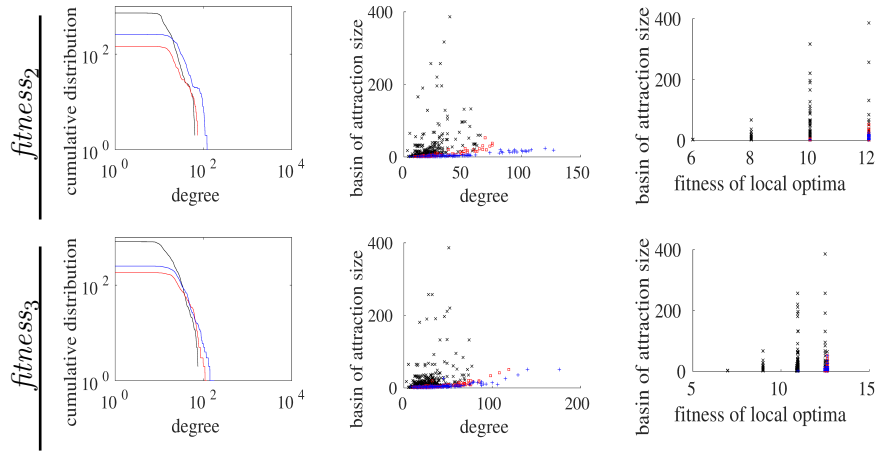


Figure .17: Statistical measures for *lex* initialization on $n = 5$ with fitness functions $fitness_2$ and $fitness_3$ for operators flip (black), insert (blue), swap (red) using 10 000 samples: Cumulative degree distribution in a log-log scale (left), Correlation between the degree of local optima and their corresponding basin sizes (middle), and Correlation between the fitness of local optima and corresponding basin sizes (right).

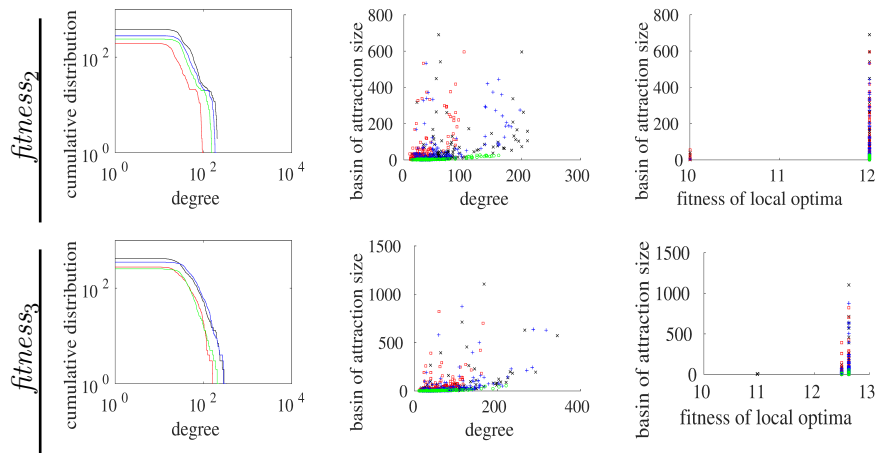


Figure .18: Statistical measures for *lex* initialization on $n = 5$ with fitness functions $fitness_2$ and $fitness_3$ for combination using operators flipinsert (black), swapflipinsert (blue), swapflip (red), and swapinsert (green) using 10 000 samples: Cumulative degree distribution in a log-log scale (left), Correlation between the degree of local optima and their corresponding basin sizes (middle), and Correlation between the fitness of local optima and corresponding basin sizes (right).

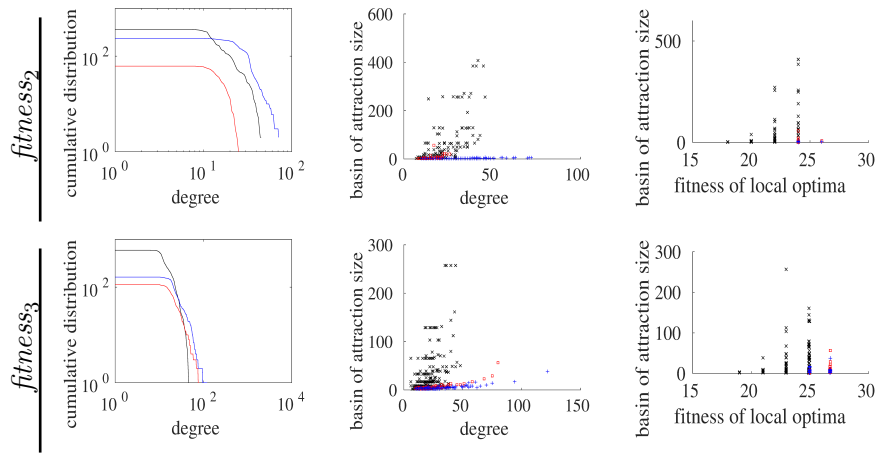


Figure .19: Statistical measures for *lex* initialization on $n = 6$ with fitness functions $fitness_2$ and $fitness_3$ for operators flip (black), insert (blue), swap (red) using 10 000 samples: Cumulative degree distribution in a log-log scale (left), Correlation between the degree of local optima and their corresponding basin sizes (middle), and Correlation between the fitness of local optima and corresponding basin sizes (right).

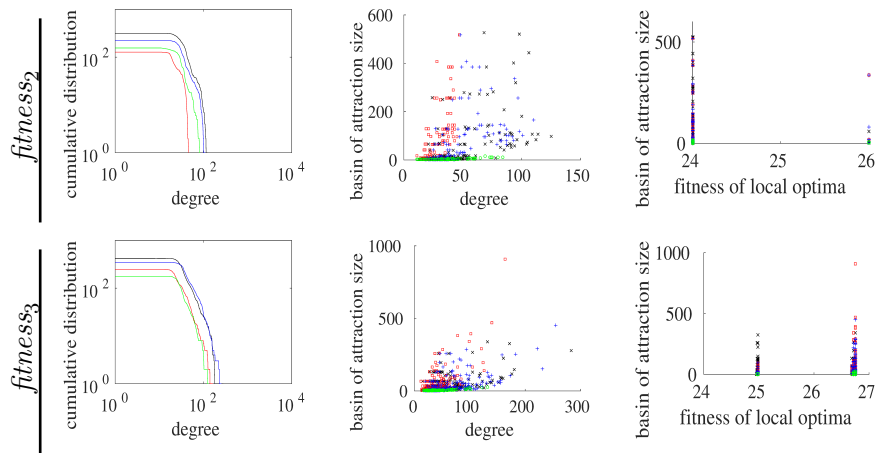


Figure .20: Statistical measures for *lex* initialization on $n = 6$ with fitness functions $fitness_2$ and $fitness_3$ for combination using operators flipinsert (black), swapflipinsert (blue), swapflip (red), and swapinsert (green) using 10 000 samples: Cumulative degree distribution in a log-log scale (left), Correlation between the degree of local optima and their corresponding basin sizes (middle), and Correlation between the fitness of local optima and corresponding basin sizes (right).